

2017

Cholinergic modulation of excitatory synapses of the ACC and LPFC

<https://hdl.handle.net/2144/23826>

"Downloaded from OpenBU. Boston University's institutional repository."

BOSTON UNIVERSITY
SCHOOL OF MEDICINE

Thesis

**CHOLINERGIC MODULATION OF EXCITATORY SYNAPSES OF THE ACC
AND LPFC**

by

CHARLES KOPP

B.S. LeTourneau University 2011

Submitted in partial fulfillment of the
requirements for the degree of
Master of Science

2017

© 2017 by
Charles Michael Kopp
All rights reserved

Approved by

First Reader

Maria Medalla, Ph.D.
Assistant Professor of Neurobiology of Cortical Circuits

Second Reader

Simon Levy, Ph.D.
Associate Professor of Physiology and Biophysics

DEDICATION

I would like to dedicate this work to my grandfather Charles Crapuchettes, his inspiration and love has been a source of strength for me throughout my life.

ACKNOWLEDGMENTS

First, I want to give glory to God for whom without, I would not be able to be where I am today. I would like to thank Dr. Maria Medalla, for allowing me the opportunity to work in such an amazing lab, Dr. Luebke and Dr. Svakumaran for their help with electrophysiology, Silas Busch and Alexander Hsu for all their help with my thesis project, and Dr. Simon Levy who has been a wonderful advisor to me during my time here at BU. I also want to thank my parents, Charles and Patricia Kopp for encouraging me to pursue my dreams and supporting me along the way. I would never have come so far if it were not for them. Finally, I would like to thank Maria Geba, for all her love and support which have been mainstays of my mental health during the challenges of these past two years.

**CHOLINERGIC MODULATION OF EXCITATORY SYNAPSES OF THE ACC
AND LPFC**

CHARLES KOPP

ABSTRACT

Acetylcholine modulates neuronal activity in the brain with different responses in activity depending on the region of the brain. Our study was focused on the cholinergic modulation of excitatory synaptic transmission in the monkey anterior cingulate cortex (ACC) and lateral prefrontal cortex (LPFC), with specific focus on the effects of carbachol, a cholinergic agonist, on spontaneous excitatory postsynaptic currents (sEPSCs) and on the expression the muscarinic cholinergic type II (M2) receptor in these regions. We used electrophysiology to analyze the effects of carbachol on sEPSC of layer 3 (LIII) pyramidal neurons from each area. We used confocal microscopy to study the M2 colocalization with axon terminals labeled with vesicular glutamate transporter 1 (VGLUT1) in the ACC and LPFC, and the colocalization of M2 with specific axon terminals from the amygdala labeled with tracer and terminating in the ACC.

Results from the electrophysiological experiments showed that both the ACC and LPFC L3 neurons responded to carbachol by decreasing the frequency of sEPSCs. Cells from the LPFC showed a decrease in sEPSC frequency after 4 minutes in carbachol, an earlier timepoint than ACC neurons, which showed a decrease in sEPSCs frequency after 6 minutes in carbachol. In the confocal studies, M2 expression and colocalization with VGLUT1 terminals in the ACC and LPFC were observed. However, we observed a greater total area of M2 expression in the ACC *versus* the LPFC in layer 1. We found

minimal colocalization of the M2 receptor with axon terminals from the amygdala in the ACC. Together, our data show that acetylcholine has distinct interactions with neurons and pathways in ACC and LPFC, which may be related to the distinct function of the two areas in cognition, learning and memory.

TABLE OF CONTENTS

TITLE PAGE	i
COPYRIGHT PAGE	ii
SIGNATURE PAGE	iii
DEDICATION	iv
ACKNOWLEDGMENTS	v
ABSTRACT	vi
TABLE OF CONTENTS.....	viii
LIST OF TABLES	ix
LIST OF FIGURES	x
LIST OF ABBREVIATIONS.....	xiii
INTRODUCTION	1
MATERIALS & METHODS	14
RESULTS	23
REFERENCES	48
CURRICULUM VITAE.....	63

LIST OF TABLES

1	Synaptic properties of sEPSCs	25
2	IEI K-S test	26

LIST OF FIGURES

Figure	Title	Page
1	Comparison of laminar structures of the ACC versus the LPFC	7
2	Layer IV pyramidal neurons	23
3	Examples traces of sEPSCs from the ACC and LPFC	24
4	Effects of carbachol on the frequency of sEPSCs in ACC <i>versus</i> LPFC	27
5	Effects of carbachol on the amplitude of sEPSCs in ACC <i>versus</i> LPFC neurons	29
6	Effects of carbachol on the area of sEPSCs in ACC <i>versus</i> LPFC neurons	30
7	Effects of carbachol on the rise-time of sEPSCs in ACC <i>versus</i> LPFC neurons	32
8	Effects of carbachol on the half-width of sEPSCs in ACC <i>versus</i> LPFC neurons	33
9	Effects of carbachol on the decay of sEPSCs in ACC <i>versus</i> LPFC neurons	34
10	ACC M2 and VGLUT1 expression	36
11	LPFC M2 and VGLUT1 expression	37

12	Particle analysis of VGLUT colocalization with M2 expression in the ACC and LPFC	38
13	Tracer injection site in amygdala to label projection terminations in the ACC	40
14	Confocal Analysis of PIJ	41
15	Confocal Analysis of PIK	42
16	Distribution of amygdala fibers in the ACC	43

LIST OF ABBREVIATIONS

ACC	Anterior Cingulate Cortex
ACh.....	Acetylcholine
AChR	Acetylcholine Receptor
AMPA.....	α -amino-3-hydroxy-5-methyl-4isoxazolepropionic Acid Receptor
AMY	Amygdala
AP	Action Potential
BU	Boston University
BDA	Biotinylated Dextran Amine
BSA.....	Bovine Serum Albumin
CCh	Carbachol
FE.....	Fluoroemerald
fMRI.....	functional Magnetic Resonance Imaging
FR.....	Fluororuby
GABA	gamma-aminobutyric Acid
GLAST.....	L-Glutamate/L-Aspartate Transporter
IHC.....	Immunohistochemistry
IEI	Inter-Event Interval
K-S test.....	Kolmogorov-Smirnov Test
LPFC.....	Lateral Prefrontal Cortex
M1	Muscarinic receptor type I
M2.....	Muscarinic receptor type II

NGS.....	Normal Goat Serum
NMDA	N-methyl-D-aspartate receptor
PB.....	Phosphate Buffer
PBS	Phosphate Buffer in Saline
PFC	Prefrontal Cortex
PMC	Premotor Cortex
REM.....	Rapid Eye Movement
sEPSC	Spontaneous Excitatory Postsynaptic Current
Tx	Triton X-100
VGLUT.....	Vesicular Glutamate Transporter
WM.....	Working Memory
YNPRC	Yerkes National Primate Research Center
+	Positive signal

Introduction

The cortex is the outer mantle of the brain that plays an important role in the control of conscious behaviors and bodily functions such as regulation of autonomic responses and emotions, coordination of voluntary movements, sensory perception, problem solving, and decision making. The mammalian cortex is comprised of different regions, which monitor and control different aspects of behavior. The cortex relays electrical and chemical signals to other brain structures through a network of neurons interconnected via synaptic connections (Kandel, et al, 2012). A neuron sends signals through firing a series of action potentials (APs). When a neuron's membrane potential reaches threshold, voltage-gated sodium channels rapidly open and a large all-or-none depolarizing spike -- the action potential-- occurs. The AP is generated in the axon hillock and travels down to the axon terminals opening voltage-gated calcium channels to trigger calcium influx for neurotransmitter release at the synaptic cleft. Neurotransmitters are released from presynaptic vesicles into the cleft, which then bind to a receptor on the postsynaptic neuron that signals channels to open or triggers a secondary messenger cascade (Nicholls et al., 2011; Kandel et al., 2012). Precisely how these individual cells in the cortex communicate in such a way to generate a certain behavior is not well understood.

Excitatory signaling in the mammalian cortex

The cortex is comprised of two primary classes of neurons: the excitatory glutamatergic neurons which depolarize and activate their targets, and the gamma-

aminobutyric Acid (GABA) secreting neurons (i.e. GABAergic neurons) that hyperpolarize and suppress activity (Markram et al., 2004). Excitatory pyramidal neurons are the most prevalent cell type of the cortex, with their role being the major projection neurons that facilitate communication from one region of the brain to another (Elston, 2003). They are characterized by a pyramidal soma with a single projecting axon that originates from the base of the soma. There are two main dendritic arbors of the pyramidal neuron: basal and apical. Pyramidal neurons generally have one large apical dendrite emanating from the apex of the soma and extending towards the pial surface. The main apical trunk travels perpendicular to the pia, and then arborizes into an apical tuft. At the base of the pyramidal soma, a skirt of basal dendrites arise and extend laterally or towards the white matter (DeFelipe & Fariñas, 1992).

Excitatory signals from a variety of sources are received by the dendrites of pyramidal neurons on dendritic spines – the thornlike protrusions that are the major postsynaptic sites for excitatory synapses. These spines have different sizes and shapes with four general classifications: thin, mushroom, stubby, and filipodia (Peters & Kaiserman-Abramof, 1970; Chang & Greenough, 1984; Hering & Sheng, 2001). Excitatory synapses on dendrites are summated in the soma, which may trigger the generation of an AP at the axon hillock located in the axon initial segment (Stuart, Schiller, & Sakmann, 1997; Golding & Spruston, 1998). To balance excitation, pyramidal neurons receive inhibitory inputs that can inhibit AP firing when sufficiently activated. These inhibitory synapses are strategically clustered throughout the pyramidal dendritic

tree, with a dense compartment of inhibitory input onto proximal dendrites, somata and the axon initial segments (Markram et al., 2004).

The cortex is a laminated structure, consisting of 3-6 layers of cells, which vary across the distinct cortical areas (Defelipe, 2011; Barbas, 2015). The layers are arranged with layer 1 positioned closest to the pia, and the rest arranged numerically going deeper into the cortex. Each layer consists of unique populations of excitatory and inhibitory neurons, and distinct inputs and outputs (Barbas, 2015). The most superficial layer 1 is mostly acellular, containing a few glial cells, inhibitory neurons, and the apical dendrites of pyramidal neurons whose somata are located in deeper layers. The middle internal granular layer 4 mostly consists of small local excitatory and inhibitory neurons and receives input from the thalamus (Jones, 1998). The distinct populations of pyramidal neurons reside mainly in the supragranular layers 2-3 and the infragranular layers 5-6, and have distinct targets. Pyramidal neurons located in layers 2-3 mainly participate in cortico-cortical communication, and a subset of those in layer 5 have a population projecting to subcortical structures, such as the thalamus (Douglas & Martin, 2004; Goodfellow, Benekareddy, Vaidya, & Lambe, 2009). In the current study, we investigate the properties of glutamatergic signaling of pyramidal neurons, specifically in layers 2-3 in two distinct prefrontal areas. We assess how these excitatory synaptic signals are modulated by acetylcholine, an important neuromodulator of cortical activity, wakefulness and consciousness.

Prefrontal Cortex

The prefrontal cortex (PFC), situated in the most rostral part of the cerebral cortex, serves a critical role in decision making and executive control that selects important information and suppresses irrelevant information for the task at hand (Miller & Cohen, 2001; Elston, 2003; Fuster, 2001). In humans and non-human primates, the PFC is highly complex and expanded, consisting of different areas that possess unique structure and function (Barbas & Pandya, 1989). In the rhesus monkey, the PFC is subdivided into three main subregions – the lateral, medial and orbital prefrontal cortices – that consist of several distinct architectonic areas (Petrides, Tomaiuolo, Yeterian, & Pandya, 2012). It is situated in the brain to receive input from a wide array of internal and external sources.

The PFC has connections with higher-order sensory areas integrating visual, somatosensory, and auditory information from the parietal, occipital, and temporal lobes. The PFC also has connections with the amygdala, hypothalamus, and hippocampus, which are integral components of the limbic system for processing long-term memory, emotions, affect, and motivation (Barbas, 2000). Communication with these various areas allows the PFC to paint a complete picture of the sensory external environment, along with our emotional state, and previous experiences to make decisions that will most likely result in beneficial outcomes (Schacter, 1997). The ability to control action for decision making relies on PFC communication with cortical and subcortical motor structures. The PFC is interconnected with the premotor cortex, supplementary motor area, the presupplementary motor area, and the rostral cingulate motor cortex, all of which are

regions involved in refining motor planning and goal oriented action (Alexander, DeLong, & Strick, 1986; Bates & Goldmanrakis, 1993). Thus, the PFC is able to gather and distribute information to many regions of the brain making it ideal for coordinating decisions and actions, which require higher level processing.

Lateral Prefrontal Cortex

The lateral prefrontal cortex (LPFC) is a subdivision of the PFC positioned on the lateral surface that plays an important role in communicating with the high-order sensory and premotor cortices (Carmichael & Price, 1995; Petrides, 2005). The premotor cortex is involved in generating goal-oriented movements, such as grasping an object, and together with the PFC is critical for carrying out decisions (Rizzolatti et al., 1988). The LPFC is involved in updating and transforming sensory-motor information, creating motor plans, shaping perception, allocating attention, and maintaining information in working memory (WM) for goal directed behavior (Fuster, 2001; Miller & Cohen, 2001). The capacity to perform time delayed tasks, like when one must remember a newly learned set of directions long enough to reach the destination, is important for the ability to operate in novel environments without having to memorize the location of everything in the surrounding area. Neurons in the LPFC are active during these working memory tasks (Funahashi, Bruce, & Goldmanrakis, 1989; 1993).

One of the central roles of the LPFC is assisting in achieving behavioral aims through the temporal assembly of information and responses (Brunia, Haagh, & Scheirs, 1985). As a new action is learned, the LPFC and premotor areas are observed to be active

in positron emission tomography (Jenkins, Brooks, Nixon, Frackowiak, & Passingham, 1994). This activity in the LPFC and premotor areas slowly decreases as the learned action becomes more instinctual and/or memorized. Activation of the LPFC seems dependent on whether the task consists of temporarily useful information that can be discarded as soon as the task is completed (Fuster, 2001).

The LPFC is arranged both in a rostral-caudal and a dorsal-lateral axis (Petrides, 2005). The most rostral portion of the LPFC, area 10, is involved in higher-order processing, especially those involving multi-tasking or decisions made between multiple options. The middle to caudal LPFC areas 9, 46, 8 and 12 (Figure 1) are involved in working memory functions – a form of short term memory for monitoring and manipulating information for a task at hand, such as temporarily remembering a verbally acquired phone number long enough to dial it (Goldman-Rakic, 1995). Lesions in the LPFC lead to a deterioration in performance of tasks which involve WM, and difficulty in verbal fluency (Owen, Downes, Sahakian, Polkey, & Robbins, 1990). Impairments in the Wisconsin Card Sort test for example, which requires an individual to sort cards with the rules of how to sort them changing frequently, may indicate damage to the LPFC (Petrides, 1994; 2005; Kandel et al., 2012). The mid-dorsolateral prefrontal cortex is involved in monitoring, while the mid-ventrolateral prefrontal cortex is more involved in the manipulation of information in WM (Petrides, 2005).

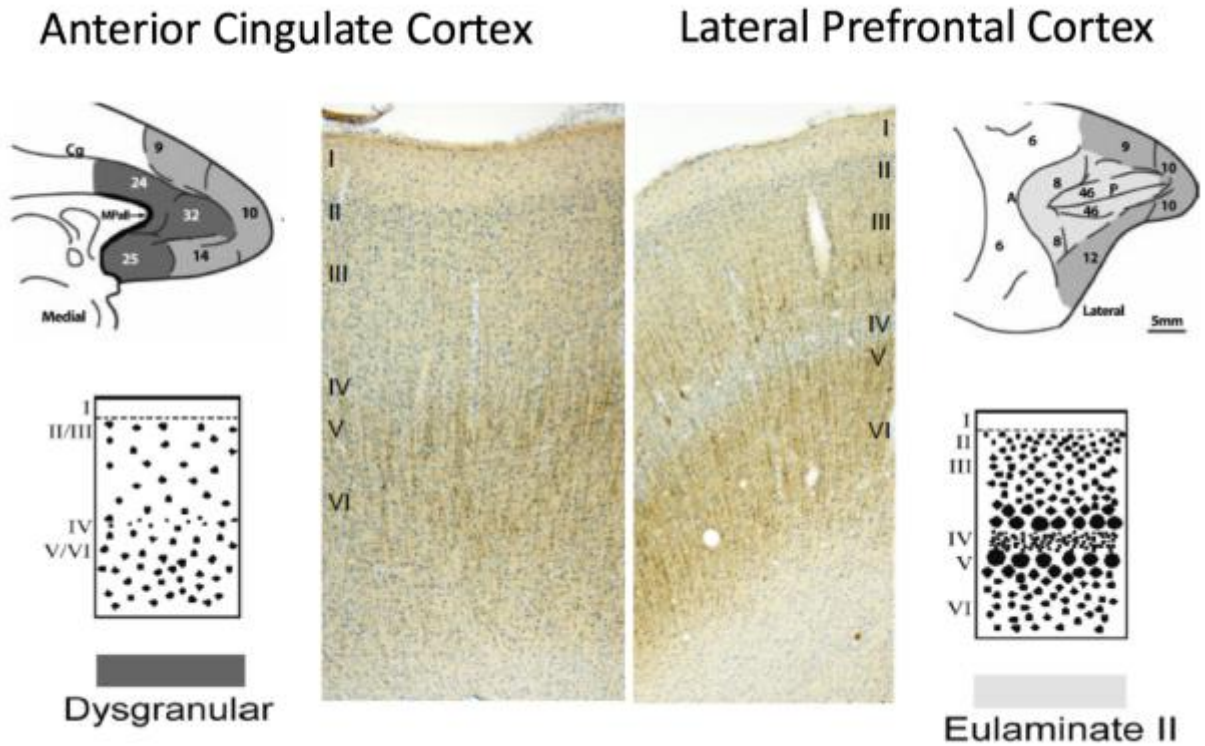


Figure 1. Comparison of laminar structures of the ACC versus the LPFC. Left: Schematic diagram of the medial surface of the monkey brain showing ACC areas 24, 25, and 32 (shaded dark gray), which is rostral to the Corpus Callosum (top). Schematic diagram (bottom) and photomicrograph of a coronal section stained with Nissl and SMI-32 (brown, marker of pyramidal neurons in layer 3 and 5); showing laminar structure of the ACC with a less defined layer IV and overall lower cell density. Right: Lateral surface of the brain showing location of LPFC area 46 (top). Schematic diagram and Nissl and SMI-stained coronal section of eulaminar LPFC area 46 showing a clearer layer II, III, and IV. Image created by Dr. Maria Medalla

The current study focuses on LPFC area 46 along the principal sulcus, as shown in Fig. 1, on the lateral surface of the monkey brain (Barbas & Pandya, 1989; Miller & Cohen, 2001; Luebke, Barbas, & Peters, 2010). It is a 6-layered eulaminar neocortical

area with a well-developed layer IV. In humans, area 46 is situated on the middle frontal gyrus. Area 46 has strong connections with the visual (parietal, parieto-occipital association, and superior temporal sulcal cortices), auditory (rostral superior temporal gyrus), and somatosensory sensory association cortices. Area 46 also possesses interconnections with the limbic retrosplenial cortex, and anterior and posterior cingulate cortices (Petrides & Pandya, 1984; Barbas & Pandya, 1989; Cavada & Goldman-Rakic, 1989; Andersen, Asanuma, Essick, & Siegel, 1990).

Anterior Cingulate Cortex

The anterior cingulate cortex (ACC), which is the rostral portion of the cingulate cortex around the corpus callosum, is a component of the medial PFC (Figure 1) (Devinsky, Morrell, & Vogt, 1995). This area is part of the Papez limbic circuit for emotions and memory (Paus, 2001). The ACC consists of dysgranular cortices with an unremarkable layer 4 (Fig. 1), and Brodmann's areas 24, 25, and 32 (Paus et al., 1996). These dysgranular ACC areas have fewer than 6 layers and lower cell density than other neocortical eulaminate areas (Barbas & Zikopoulos, 2007).

The ACC has two major anatomical regions, the ventral-rostral portion which contains areas 24a, b, & c, 25, and 32, while dorsal-caudal area is composed of areas 24b, 24c, and 32 (Barbas & De Olmos, 1990; Barbas & Blatt, 1995). These major anatomical regions are thought to correspond to two main functional regions of the ACC: the ventral-rostral "affect" region and dorsal-caudal "cognition" region (Paus, 2001). The ventral ACC areas associated with the "affect" region (areas 25, 32, and ventral anterior parts of

area 24) have strong connections with the amygdala and brainstem motor nuclei. These structures participate in the regulation of the endocrine system, emotional learning, and ascribing emotional importance to internal thoughts and external stimuli.

Correspondingly, the hippocampus and amygdala, limbic structures crucial for memory and emotions respectively, both send projections to the ventral rostral part of the ACC (Barbas & De Olmos, 1990; Devinsky et al., 1995). The dorsal caudal portion (area 24) is associated the “cognition” region, which compared to the “affect” region has stronger connections with premotor cortices and the LPFC (Petrides, 2005). This “cognition” ACC region continues posteriorly as the mid-cingulate cortex that projects directly to the motor cortex and the cervical section of the spinal column (Dum & Strick, 1991; Paus, 2001).

The ACC integrates motor control, cognition, and arousal state information to guide decision making (Paus, 2001). The ACC is implicated in behavioral tasks, which require greater cognitive load, in evaluating emotion and cognitive changes, and in pain modulation (Kennard, 1955; Corkin, 1979; Pardo, Pardo, Janer, & Raichle, 1990).

Additionally the ACC plays a role in modulating arousal state because of connections with hypothalamic and brainstem centers for arousal such as the ventral tegmentum area and locus coeruleus (Berger, 1992; Rempel-Clower & Barbas, 1998; Aston-Jones & Cohen, 2005). It also has strong associations with the medial temporal and hippocampal structures which are important for long-term memory and expression of emotion (Barbas & Zikopoulos, 2007). The ACC’s projections to premotor and cingulate motor areas

allow it to play a role in movement (Luppino, Matelli, Camarda, Gallese, & Rizzolatti, 1991).

Similar to the LPFC, the ACC plays an important role in the decision-making process. The ACC has strong connections with the LPFC, which originate in layer V and terminate in the upper layers of the LPFC; this connection is important for executive control and decision making (Barbas & Pandya, 1989; Posner & Dehaene, 1994; Rushworth, Walton, Kennerley, & Bannerman, 2004; Medalla & Barbas, 2009, 2010). For example, the ACC is shown to have strong functional magnetic resonance imaging (fMRI) activation when making a decision using incongruent stimuli presented during a Stroop test (Pardo et al., 1990). In the Stroop test, participants are instructed to select the color of the words rather than read the names of the colors. If the stimuli are congruent (i.e. the word “red” is written in red), there is no conflict and the participant is able to identify the color of the word easily. If the stimuli are incongruent (i.e. “red” is written in blue), this prompts an individual to read the word rather than identify the color the word is written in. Dysfunction in the ACC can lead to neurological disorders, such as schizophrenia, that are characterized by impairments in cognitive-emotional integration (Devinsky et al., 1995). However, how the ACC is unique compared to other PFC areas in terms of its role in behavior, and its underlying circuitry, is largely unknown especially in primates. The focus of this study is to compare how the ACC differs from LPFC with regards to excitatory circuits and modulation by acetylcholine.

VGLUT Transporters

Glutamate is a pervasive amino acid that plays a critical role in excitatory signaling in the brain. When glutamate is released into the synaptic cleft by the presynaptic terminal it binds to the AMPA receptor and allows Na^+ in and K^+ out of the postsynaptic terminal. When this is coupled with an EPSC, which removes Mg^{2+} from blocking the N-methyl-D-aspartate (NMDA) receptor, it causes a sharp rise in Ca^{2+} in the postsynaptic cell. Thus, these receptors assist in the changing of a biochemical signal into an electrical signal (Kandel et al., 2012).

The VGLUT family of transporters are highly specific to the packaging and transport of glutamate. When glutamate is released into the synaptic cleft, it is taken up by glial cells through the GLAST receptor and converted into glutamine (Hamberger, Chiang, Nylén, Scheff, & Cotman, 1979; Shigeri, Seal, & Shimamoto, 2004). The glutamine is then released out of the glial cell and uptaken at the presynaptic terminal and converted back to glutamate by the VGLUT family of transporters (Shigeri et al., 2004). These transporters require a proton gradient, maintained by a H^+ ATPase, and low concentrations of Cl^- to function properly (Ozkan & Ueda, 1998).

VGLUT1 & VGLUT2 are two subtypes of glutamate transporters which have unique distributions in the brain. The cerebral cortex, hippocampus, and cerebellum primarily express VGLUT1 except in layer 4 in the neocortex which has increased expression of VGLUT2 (Fremeau Jr, Voglmaier, Seal, & Edwards, 2004). While there is no consensus on how these two transporters differ in their treatment of glutamate transport and packaging, VGLUT2 appears to be expressed more on neurons that

experience higher quantities of transmitter release (Hessler, Shirke, & Malinow, 1993; Rosenmund, Clements, & Westbrook, 1993)

Cholinergic Signaling in the Cortex

The activity of excitatory and inhibitory neurons in the cortex are modulated by a variety of monoaminergic and catecholaminergic neurotransmitters (Kandel et al., 2012). Among these, acetylcholine (ACh) is an important neuromodulator of cortical activation, oscillatory states, and synaptic transmission. Cholinergic fibers in the cortex and hippocampus arise from neurons of the basal forebrain nuclei (Nicholls et al., 2011). The cholinergic system is essential for learning, memory, and cognition (Dunnett, Everitt, & Robbins, 1991). Increasing availability of ACh in the synaptic cleft, by inhibition of Acetylcholinesterase (AChE), which breaks down ACh, leads to improvement in memory and learning (Nicholls et al., 2011).

There are two major classes of cholinergic receptors in the CNS: nicotinic and muscarinic (Levey, Kitt, Simonds, Price, & Brann, 1991). In the cortex, ACh acts primarily on muscarinic receptors, the predominant subtype in the cortex. Muscarinic receptors are G-protein coupled receptors, which consist of distinct pharmacological subtypes based on subunit composition. The muscarinic type I (M1) pharmacological subtype, which contain the m1 or m3 subunits, is the predominant subtype. The M1 receptor subunit is the most dense in the cortex, and is mainly located postsynaptically on spines of pyramidal neurons (Levey et al., 1991). Activation of M1 receptors cause

depolarization of pyramidal neurons through secondary messengers and leads to the opening of calcium channels (McKinney, 1993).

The muscarinic type 2 (M2) receptor is a G-protein coupled receptor, predominantly located on the presynaptic bouton (Levey et al., 1991; Guerram, Zhang, & Jiang, 2016). When acetylcholine is released into the synaptic cleft, M2 receptors provides an inhibitory effect on excitatory feedback synapses (Hasselmo & Schnell, 1994). This inhibition is caused by a deactivation of adenylyl cyclase, which leads to the weak activation of phosphatidylinositol-4,5 bisphosphate hydrolysis (Peralta, Ashkenazi, Winslow, Ramachandran, & Capon, 1988; Levey et al., 1991). The downstream effects of this process have not been described.

Cholinergic modulation plays an important role in several regions of the brain including the hippocampus, neocortex, thalamus, PFC and cingulate cortex (Krnjević & Phillis, 1963; Krnjević, Pumain, & Renaud, 1971; Hasselmo, 1995, 2006). The action of acetylcholine reduces the level of signal to noise ratio in the hippocampus and PFC (Hasselmo, 1995 ;Bunce, Sabolek, & Chrobak, 2004). ACh also participates in visual attention and discrimination learning in primates by acting in the hippocampus, perirhinal cortex, and cingulate cortex; this has been demonstrated in lesion studies which remove cholinergic innervation (Dunnett et al., 1991). Patients with Alzheimer Disease have shown marked improvement in memory when given cholinergic agonists (Everitt & Robbins, 1997).

Acetylcholine modulates activity of neurons through muscarinic receptors but whether its action increases or decreases firing of AP or sEPSCs on specific neural

pathways is not known. Interestingly, the levels of acetylcholine is highest during waking hours and during REM sleep states (Chrobak & Buzsáki, 1994; Hasselmo, 1999). The LPFC and ACC show marked differences during REM sleep: The LPFC remains inactive during REM while the ACC is activated, which parallels an increase in acetylcholine in the brain (Muzur, Pace-Schott, & Hobson, 2002). Anatomic data show that M2 receptors were found to be in higher percentages on boutons from ACC axons terminating in LPFC, suggesting a mechanism that can suppress communication between ACC to LPFC (Medalla & Barbas, 2012). Compared to the LPFC, the ACC is more heavily innervated by cholinergic fibers (Mesulam, Mufson, Levey, & Wainer, 1983). The different role of acetylcholine in the primate ACC, and specifically how it differs from other prefrontal areas such as the LPFC, is not well understood and is the focus of this study.

MATERIALS AND METHODS

Experimental subjects

Boston University obtained 10 rhesus monkeys (*Macaca mulatta*); (males 5-7 years) from Yerkes National Primate Research Center (YNPRC) at Emory University in Atlanta. These monkeys were kept in the Laboratory Animal Science Center at Boston University School of Medicine (BUSM) under a 12-hour light and dark cycle. Both the YNPRC and BUSM are fully accredited by the Association for Assessment and Accreditation of Laboratory Animal Care. The recommendations of the National Institutes of Health *Guide for the Care and Use of Laboratory Animals* and the *U.S. Public Health Service Policy on Humane Care and Use of Laboratory Animals* were followed scrupulously (National Research Council (US) Committee for the Update of the *Guide for the Care and Use of Laboratory Animals*, 2011).

Preparation of acute slices for recording

To retrieve brain tissue, monkeys were sedated with ketamine hydrochloride (10 mg/ml). Once sedated, they were heavily anesthetized with sodium pentobarbital (15 mg/kg, IV). The craniotomy was performed on the monkeys as previously described (Amatrudo et al., 2012; Luebke & Amatrudo, 2012). A thoracotomy was performed, then monkeys were perfused via the ascending aorta with cold Krebs-Henseleit buffer (concentrations in mM: 6.4 Na₂HPO₄, 1.4 Na₂PO₄, 137 NaCl, 2.7 KCl, 5 glucose, 0.3 CaCl₂, 1 MgCl₂, pH 7.4; Sigma-Aldrich).

Tissue blocks were obtained from the lateral prefrontal area 46 and the anterior cingulate cortex area 24. They were quickly transferred (< 3 min) to Ringer's solution (concentrations in mM: 26 NaHCO₃, 124 NaCl, 2 KCL, 3KH₂PO₄, 10 glucose, 1.3 MgCl₂, pH 7.4; Sigma-Aldrich) and sectioned into 300- μ m-thick coronal slices with a vibrating microtome (Leica, Buffalo Grove, IL). These slices were then placed in Ringer's solution at room temperature. After the fresh tissue was harvested, the rest of the brain was perfused with 4% paraformaldehyde in 0.1M PB. Once the brains were removed from the monkeys, they were cryoprotected by placing them in solutions of sucrose (10-30%) and frozen in -70°C isopentane (Rosene, Roy, & Davis, 1986).

Electrophysiological analyses of spontaneous EPSCs of layer 3 pyramidal neurons

After equilibrating for one hour, the tissue slices were deposited in submersion-type recording chambers (Harvard Apparatus, Holliston, MA) mounted on the stages of a confocal microscope (Leica, Buffalo Grove, IL). Six slices from ACC area 24, two slices from ACC area 32, and four from LPFC area 46 were then run through a series of standard tight-seal, whole cell patch clamp recordings using layer 3 pyramidal neurons via the guidance of infrared differential interface contrast (IR-DIC) optics (Amatrudo et al., 2012). The pipettes were pulled on a horizontal Flaming and Brown micropipette puller (Model P—87, Sutter Instruments, Novato, CA) from borosilicate glass (Sutter Instruments, Novato, CA). The recording pipettes were filled with a potassium methanesulfonate-based internal solution (concentrations, in mM: 122 KCH₃SO₃, 2 MgCl₂, 5 EGTA, 10 NaHEPES, with 1% biocytin, pH 7.4; Sigma-Aldrich). The

electrodes had resistances of 3-6 M Ω with a tip of 1 μ m for optimal recording, in the external Ringer's solution. Data was collected via PatchMaster acquisition software on EPC-9 or EPC-10 patch-clamp amplifiers (HEKA Elektronik, Holliston, MA). The signal for each cell was low pass filtered at 10 kHz, with each cell monitored for access resistance during each run.

Spontaneous excitatory postsynaptic currents (sEPSCs) were recorded for a one to two-minute period, while holding the cell at -80 mV. This interval served as control for each cell. The cholinergic agonist, Carbachol (CCh), was applied in the bath (10 μ M), and sEPSCs were recorded in the continuous presence of CCh for at least six minutes. The data was loaded from PatchMaster to FitMaster (HEKA Elektronik, Holliston, MA) and finally exported to MiniAnalysis (Synaptosoft, Decatur, GA). The event detection threshold was set at the maximum root mean squared noise level (5 pA). Events were identified based on a clear fast rise time and decay time longer than 3ms.

The sEPSCs from each cell were analyzed using manual selection tools, using consistent block (40-50) and scale settings. Each event was selected by clicking on a trace which deviated from the baseline using the criteria listed above. Other criteria for excluding possible events included too much noise and bad access to the cell causing large deviations in the trace.

The events were separated into two minute intervals for analysis in groups 1-4. Group 1 was the control group where no carbachol had been present. Groups 2-4 were each a two-minute section after the administration of the carbachol, continuing to eight minutes in group 4. Frequency, mean amplitude, and mean area of all events per

group/cell were obtained. A scaled average trace of all events from each group/cell was acquired and fitted to a single exponential function to measure mean Rise time, Decay time constant (Tau1), and Half-width. Population histograms for amplitude, rise time 10-90%, and decay time 90-37% for each group in each cell were obtained. A K-S test was used on inter-event interval (time-elapsd between each event) to determine if the CCh shifted the population distribution of the events per cell. Time histograms showing the number of events from 0-8 minutes was obtained to see the effects of CCh over time.

Surgical injection of neural tracers

In two rhesus monkeys (cases PIK and PIJ, male, age = 6 y), neural tracers were surgically injected prior to perfusion of label pathways. Neural tracers were injected using MRI, surgical, and tissue processing, as previously described (Medalla, Lera, Feinberg, & Barbas, 2007; Medalla & Barbas, 2009). Using stereotaxic coordinates from the MRI scans, the injections were able to be determined while using the midline and betadine-filled ear-bar tips for reference. Injection of 3 μ L of 10 kDa fluoremerald (FE, case PIJ; dextran fluorescein, Life Technologies) or fluororuby (FR, case PIK; dextran tetramethylrhodamine) anterograde tracer was placed in the basolateral nucleus of the amygdala, using a Hamilton syringe mounted on a Microdrive. After a 18-21 day survival period, animals were perfused with paraformaldehyde as described above (Amatrudo et al., 2012).

Tissue processing for immunohistochemical procedures

After perfusion with paraformaldehyde, the whole right hemisphere was extracted from the skull, cryoprotected in increasing concentrations of glycerol, flash frozen in isopentane as described previously (Rosene et al., 1986). Sections were cut at the coronal plane into series of 30 or 60 μm using a sliding freezing microtome (American Optical, Buffalo, NY). Coronal sections through LPFC area 46 and ACC area 24 were selected based on maps of Barbas and Pandya (1989) for immunohistochemical analyses. Some tissue was obtained from the archived collection of Dr. Douglas Rosene, BUSM.

To view the M2 receptors together with presynaptic markers on tracer-labeled boutons in a light microscope we used immunohistochemistry (IHC). The tissue was washed in phosphate-buffered saline (PBS) which begins clearing out the fixative from the tissue. The tissue was then placed in 50 mM Glycine in 0.01 PBS for 60 minutes which facilitates the removal of aldehydes in the tissue from the fixative. Another wash was done with PBS followed by an antigen retrieval step where we incubate the tissue in sodium citrate at 50-60°C in a water bath. We then incubated the tissues in blocking solution of 5% normal goat serum (NGS), 5% bovine serum albumin (BSA), and 0.2% Triton X-100 (Tx). After this preblock step, the tissue is co-incubated in the following combination of primary antibodies (diluted 0.1M phosphate buffer (PB) with 0.2% BSA, 1% NGS, and 0.1% Tx solution): rat anti-M2 (1:500; Millipore, Billerica, MA) to label the M2 muscarinic receptor subtype, together with either rabbit anti-vesicular glutamate transporter 1 (VGLUT1; 1:1000; Millipore, Billerica, MA) to label a broad population of presynaptic boutons, or mouse anti-FE (1:800, Jackson Immunoresearch, West Grove,

PA) or rabbit anti-FR (1:800; Life Technologies, Carlsbad, CA) to label amygdala fibers from surgical tracer injection. The tissue is incubated in this solution first in the microwave (at 150W MW for 10mins; Ted Pella, Redding, CA) to aid with tissue penetration, and then for 48 hours at 4°C.

The tissue is then washed in 0.01M PBS (three times for 10 minutes each) and incubated in the following secondary antibodies: donkey anti-rat Alexa 647, together with either goat anti-mouse or anti-rabbit Alexa 488 or 546 (Life Technologies, Redding, CA) for VGLUT1 or FE or FR. Secondary antibodies were diluted in 0.1M PB with 0.2% BSAc, 1% NGS, and 0.1% Tx solution, and sections were incubated for 10min at 150 W in the microwave then overnight at 4°C. The tissue is washed three times in 0.1M PB, which helps eliminate excess salt from the PBS which will cause autofluorescence. The tissue is mounted on a coverslip with *Prolong antifade* and allowed to cure in a dark area for two to three days for thin sections (50µm) and up to one week for thick sections (300µm). They are stored at 4°C during this time.

Analyses of M2 label distribution and colocalization with VGLUT1 presynaptic boutons in the cortex

Multichannel confocal scans of 1-2 fields in layers 1, and 2-3 of LPFC area 46 and ACC area 24 were obtained (n=5) using a 40x, 1.3 N.A. oil immersion and a Zeiss 710 (0.07 x 0.07 x 3 µm voxel) or Leica SPE confocal microscope (0.08956 x 0.08956 x 0.34 µm voxel). Confocal stacks were deconvolved using AutoQuant (Media Cybernetics, Rockville, MD) to reduce signal blurring in the z-plane. Deconvolved

images were imported into ImageJ, then split into single channels of M2 labeling and VGLUT1 labeling. The signal to background noise ratio was modified for each channel using the threshold tool for optimal analysis of colocalization. In each section of the image stack, the density of M2 labeling in the neuropil was assessed using the particle analysis function of ImageJ (<http://imagej.nih.gov/ij/>, 1997-2016; RRID:SCR_003070; Rasband, 1997-2016; Schneider et al., 2012). Labeled particles between 0.04-2 μm^2 were marked and quantified as the fractional area covered (as a fraction of the total sampled site) by labeled puncta in each confocal stack (n =5 for each area).

To quantify overall fluorescence overlap between M2 and VGLUT1 staining in each area, ImageJ co-localization plug-in was used to mark co-localized pixels across the confocal stack, as described (Medalla and Luebke, 2015). The colocalization between the two channels -- the pixels where saturated label from each channel were found-- were marked as white. Particle analysis of this mask of white co-localized points was employed as above.

Analysis of M2 colocalization with Amygdala pathways in the ACC

Confocal images of 60 μm sections of labeled tissue for M2 receptors and amygdala terminations in the ACC were obtained (40x, oil immersion; 0.08956 x 0.08956 x 0.34 μm voxel) from 3 fields through the upper layers of the cortex in the ACC area 24: LI, LII, and LIII (n=2). The confocal microscope uses multiple lasers to visualize three distinct labeled proteins in area 24: M2 was labeled with alexa 647 (far red

channel), axonal boutons from the amygdala were labeled with either alexa 546 for case PIK (red channel), or alexa 488 for case PIJ (green channel).

These scans were exported to ImageJ where they were split into three channels: each channel was analysed independently for optimal thresholding. The colocalization between M2 channel and each of the two pathways was detected using the colocalization plug-in in ImageJ, as above. These final files are transferred to Reconstruct (SynapseWeb) where we manually counted colocalization of M2 with each pathway on individual boutons from each pathway colocalized with M2. The data was normalized as either a proportion of total boutons per layer, the proportion of M2 positive signal (M2+) on boutons per layer, or the M2+ boutons as a proportion of the total boutons in each layer.

Statistical Analysis

The data sets acquired from the electrophysiological experiments were analysed using a two-tailed t-test using averages per time point per area: control, two minutes of CCh, 4 minutes of CCh, and 6 minutes of CCh for both the ACC and LPFC. A K-S test for each statistic of every cell was run between groups 1 and 4 to test if there was a significant difference between the empirical and cumulative distributions. Histograms of each synaptic variable were obtained to see if the distribution of the frequency of events or characteristics of those events shifted after the effects of carbachol.

RESULTS

Electrophysiological analysis of sEPSCs of pyramidal neurons from the ACC and LPFC

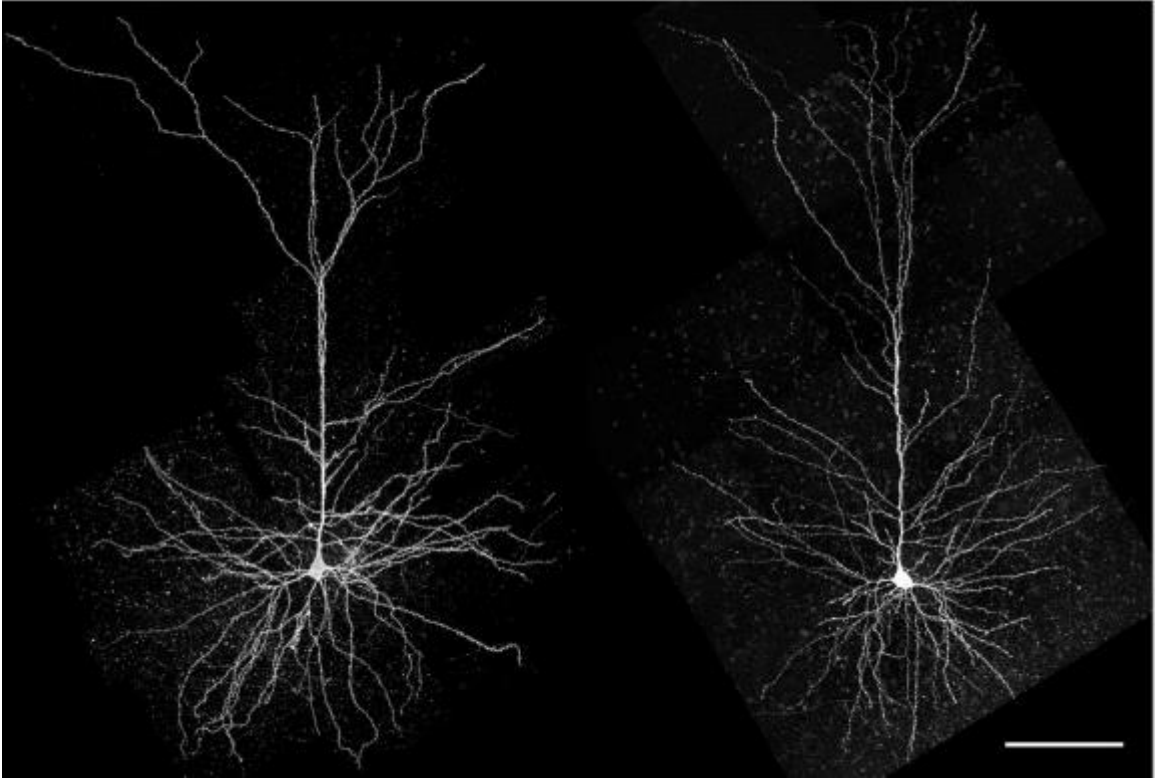


Figure 2. Layer IV Pyramidal Neurons. Left: Example of a pyramidal neuron from the ACC. Right: Example of a pyramidal neuron from the LPFC. Images created by Dr. Maria Medalla.

Whole cell patch clamp recordings were obtained from layer 3 (LIII) pyramidal neurons in ACC (n=5 from 3 animals) and in LPFC (n=4, from 3 animals) (Fig. 2). The traces of action-potential dependent, AMPA-mediated spontaneous postsynaptic excitatory currents (sEPSCs) were recorded from pyramidal neurons from area 24 in the ACC and area 46 in the LPFC. Illustrated below are example sEPSC traces from the control group, two to four minutes of CCh group, and four to six minutes of CCh group

(figure 3). Averages of each synaptic variable (frequency, amplitude, area, rise-time, half-width, and decay-time) were obtained from the individual cells and compared between the two areas.

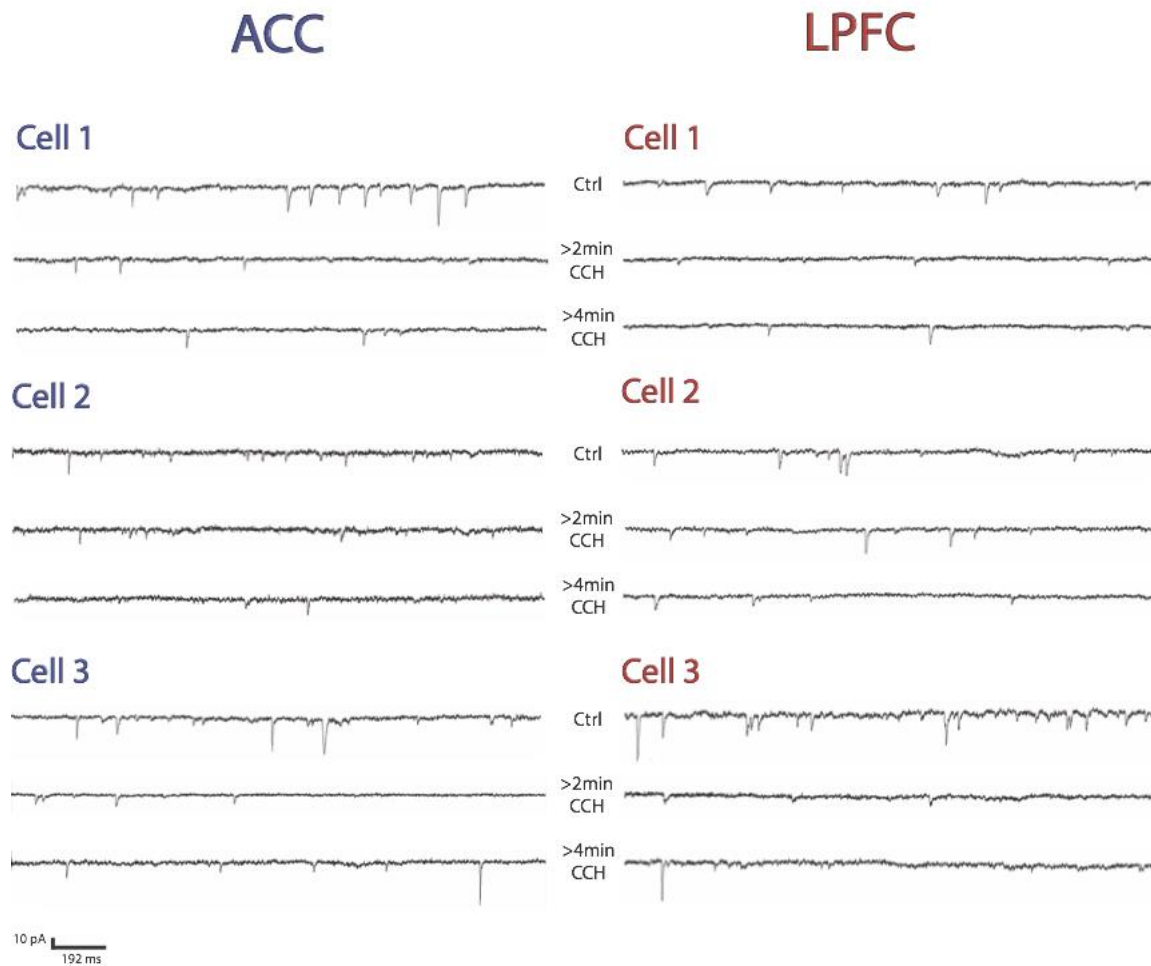


Figure 3. Example sEPSC traces of cells from the ACC and LPFC. Effect of CCh on three cells from both the ACC and LPFC. The first trace of each cell is an example trace of regular activity of a neuron in the two regions. The second and third traces represent the effects of CCh after the two and four-minute mark respectively.

Cortical Area	Group	Averages								
		n events	Hz	Amp	Decay	Area	Rise	Half width	Tau1	Decay
ACC	Ctrl	206	1.91	12.57	5.55	73.38	1.49	6.36	6.19	4.74
	0-2 min CCh	175	1.44	12.52	5.58	68.60	1.63	6.92	6.30	5.03
	2-4 min CCh	155	1.15	12.25	6.08	76.46	1.80	6.99	6.38	5.46
	4-6 min CCh	106*	0.88	12.04	6.18	69.78	1.93	7.05	6.03	5.38
LPFC	Ctrl	221	2.20	13.81	6.02	78.46	1.46	6.75	5.54	4.76
	0-2 min CCh	159	1.47	11.84	5.61	62.23	1.47	6.38	5.11	4.65
	2-4 min CCh	103*	0.95	13.60	5.41	69.54	1.52	6.04	5.15	4.76
	4-6 min CCh	104*	0.96	0.98	11.32	59.20	1.58	1.64	6.15	5.48

Table 1. Synaptic properties of sEPSCs. Averages of each area's event statistics separated by group. (*=p<0.05)

The neurons from the two prefrontal areas were similar in their properties of sEPSCs. In both the ACC and LPFC, CCh significantly decreased the number of synaptic events across time (Figure 4A, repeated measures anova $p < 0.05$ for number of events across time bins). After two minutes in CCh, we observe a decrease in the mean number of events compared to control in both ACC (control = 206 ± 49.23 number of sEPSC events, 2-4 mins in CCh = 155 ± 35.74) and LPFC (control = 221 ± 54.14 number of sEPSC events, 2-4 mins = 103 ± 27.21). In the 4 to 6 min in CCh time bin, neurons from both the ACC (106 ± 9.36 number of sEPSC events) and LPFC (104 ± 30.99 number of sEPSC events) showed a significant decrease in the mean number of events compared to control ($p=0.05$ and $p=0.02$ respectively).

To calculate the frequency of sEPSC events across time, we binned the data into four time groups: control, 0-2mins in CCh, 2-4mins in CCh, 4-6mins in CCh. Carbachol application decreased the frequency of events in both ACC and LPFC neurons (Figure 4B). However, this decrease in frequency occurred earlier in LPFC neurons than in ACC

neurons. A significant decrease in frequency of sEPSCs was observed after 2 min in CCh in LPFC (ctrl vs 2-4min CCh $p = 0.01$) and after 4mins in CCh in ACC neurons (ctrl vs 4-6 min CCh $p = 0.03$). During 2-4 min CCh group the frequency of synaptic events in LPFC neurons ($0.95 \text{ Hz} \pm 0.49$) decreased to less than half the frequency in the control group. During 4-6 minutes in CCh group, the frequency of events in both the ACC ($0.88 \text{ Hz} \pm 0.19$, $p=0.03$) and the LPFC ($0.96 \text{ Hz} \pm 0.28$, $p=0.02$) neurons were significantly lower compared to control.

K-S test IEI				
Areas	Cell #	K-S p-value	# of events Ctrl	# of events 4-6 min CCh
ACC	Cell 1 ***	0	183	77
	Cell 2 ***	0	466	141
	Cell 3 ***	0	308	129
	Cell 4 ***	0.0002	204	119
LPFC	Cell 1 ***	0	236	110
	Cell 2 ***	0	214	40
	Cell 3 ***	0	362	117
	Cell 4 **	0.0037	261	208

Table 2. IEI K-S test. A K-S test was performed on inter-event intervals on four cells from the ACC and four from the LPFC. (**= $p<0.01$ ***= $p<0.001$)

Inter-event interval (IEI) describes the time between events in a cell. After application of CCh in each cell, the population of sEPSCs based on IEI showed a greater percentage distribution toward events with longer inter-event intervals both in the ACC and LPFC neurons (Figure 4D and E). A K-S test was performed on each cell comparing the IEI in the control group with the four to six minute of CCh group (Table 2). This test shows the probability of overlap between the distributions of event-intervals times.

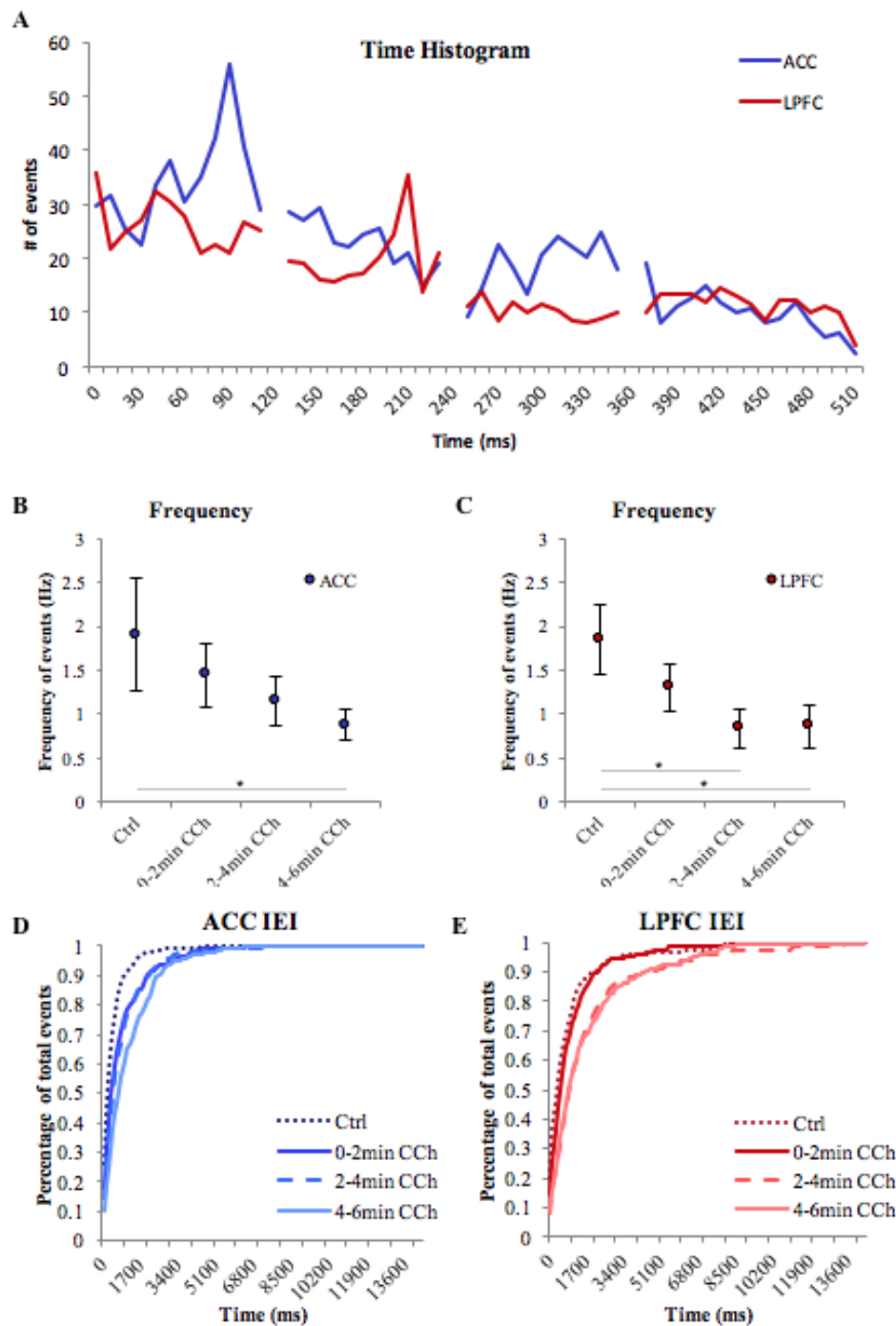


Figure 4. Effects of carbachol on the frequency of sEPSCs in ACC versus LPFC neurons. (A) The number of events across time from control to 6 mins after application of carbachol; gaps represent separation of groups: Ctrl, 0-2 min CCh, 2-4 min CCh, and 4-6 min CCh. (B, C) Mean frequency of events in ACC and LPFC neurons. (D) Normalized cumulative frequency showing the population distributions inter-event interval between groups in ACC and (E) LPFC neurons.

The mean amplitudes and area of sEPSC events was not affected by application of CCH in the ACC and LPFC neurons (Figures 5 and 6). The population distribution of amplitudes and area of sEPSCs in the ACC and LPFC neurons did not differ significantly (Figures 5B & C and 6B & C). However, consistent with the decrease in the frequency of synaptic events 2-6min after CCh, there was an overall decrease in the number events across the full distribution of amplitudes and areas.

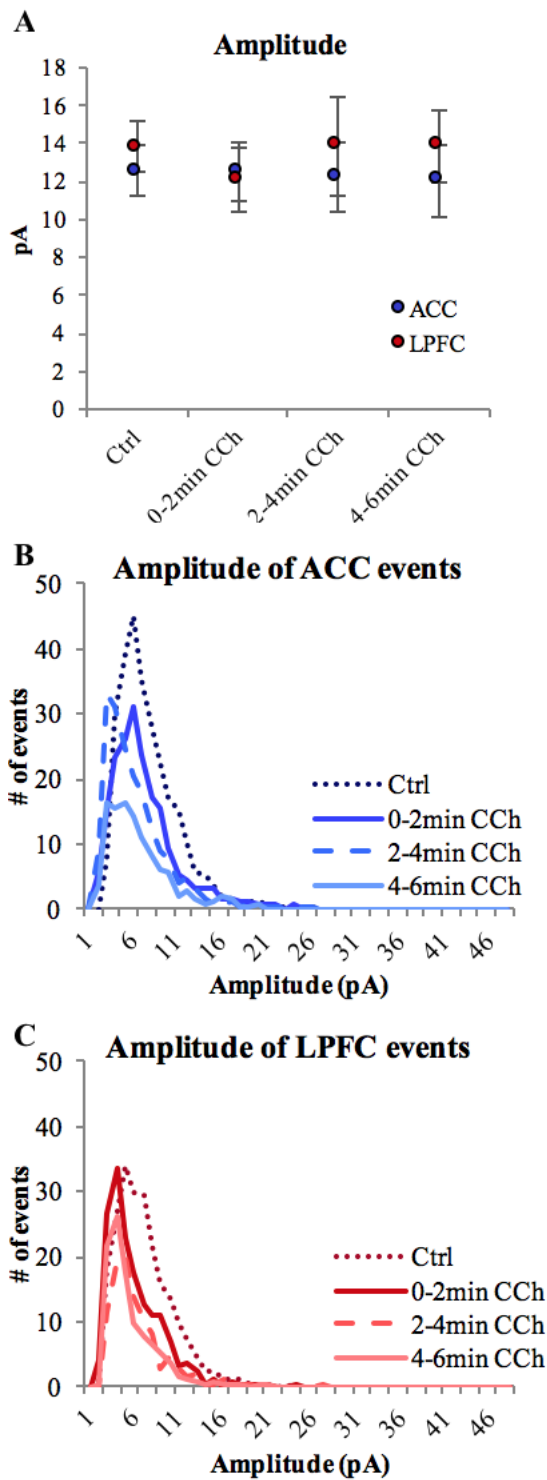


Figure 5. Effects of carbachol on the amplitude of sEPSCs in ACC *versus* LPFC neurons. A) Mean amplitude of Ctrl, 0-2 min CCh, 2-4 min CCh, and 4-6 min CCh comparing ACC (blue) and LPFC (red). Population distribution of sEPSCs events' amplitudes displaying effects of CCh with respect to the ACC (B) and LPFC (C)

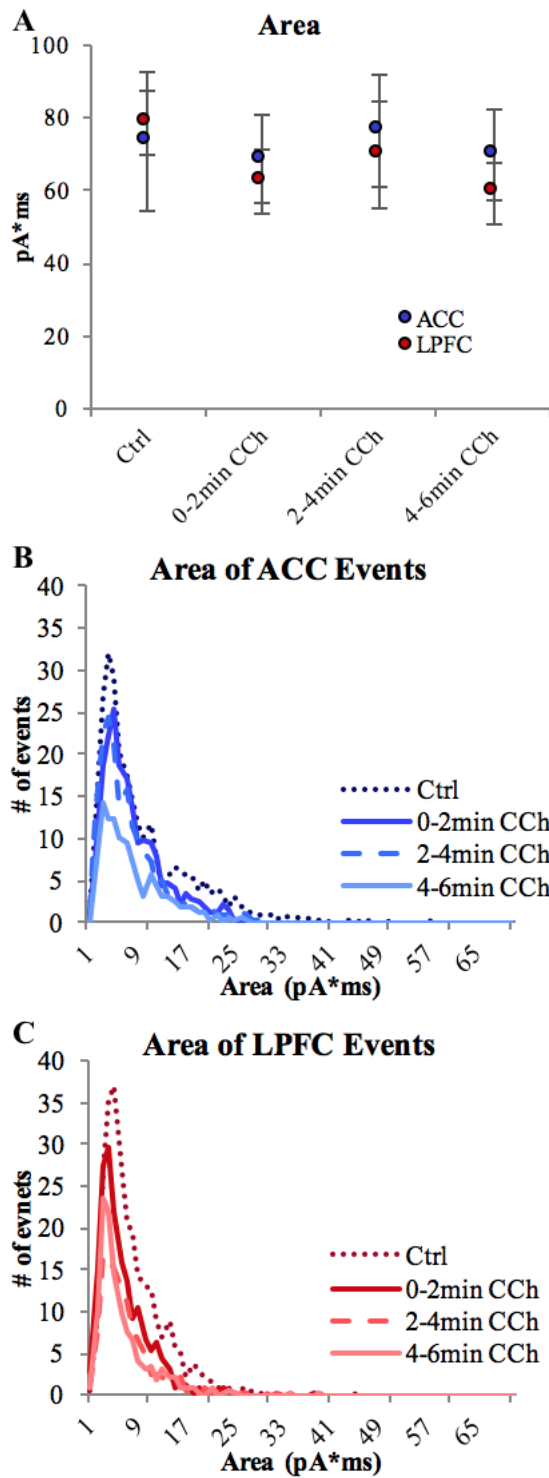


Figure 6. Effects of carbachol on the area of sEPSCs in ACC versus LPFC neurons. (A) Mean area of Ctrl, 0-2 min CCh, 2-4 min CCh, and 4-6 min CCh groups comparing ACC (blue) and LPFC (red) areas. Population distribution of sEPSCs events' areas showing effects of CCh for the ACC (B) and LPFC (C).

Similar to amplitude and area, the kinetics of sEPSCs were similar between ACC and LPFC neurons (Figures 7-9) . Carbachol has no significant effect on the kinetics of these events. The rise-time of the control groups for the ACC and LPFC ($1.49\text{ms} \pm 0.19$ and $1.46\text{ms} \pm 0.09$ respectively) were very similar (Figure 7A). However, there was a slight trend for a longer rise-times after 4-6mins in CCh compared to the control group in ACC neurons ($1.93\text{ ms} \pm 0.17$; $p = 0.09$). There was no significant change in the population distribution after the application of CCh (Figure 7B & C). As with amplitude and area, we observed a proportional decrease in the distribution of all event rise-time bins.

Half-width times of sEPSCs were largely similar between areas, and no significant effect of CCh was seen. Mean half-width times saw no significant change after CCh application (Figure 8A). Population distribution of half width times were similar between the control group and the three groups with different time in CCh (Figure 8B & C).

Decay times of sEPSCs displayed no differences between the ACC and LPFC before or after CCh administration. Mean decay times saw no change between the control group and the timed CCh groups (Figure 9A). Population distribution saw a uniform decrease in events of all decay times over the course of CCh treatment (Figure 9B & C).

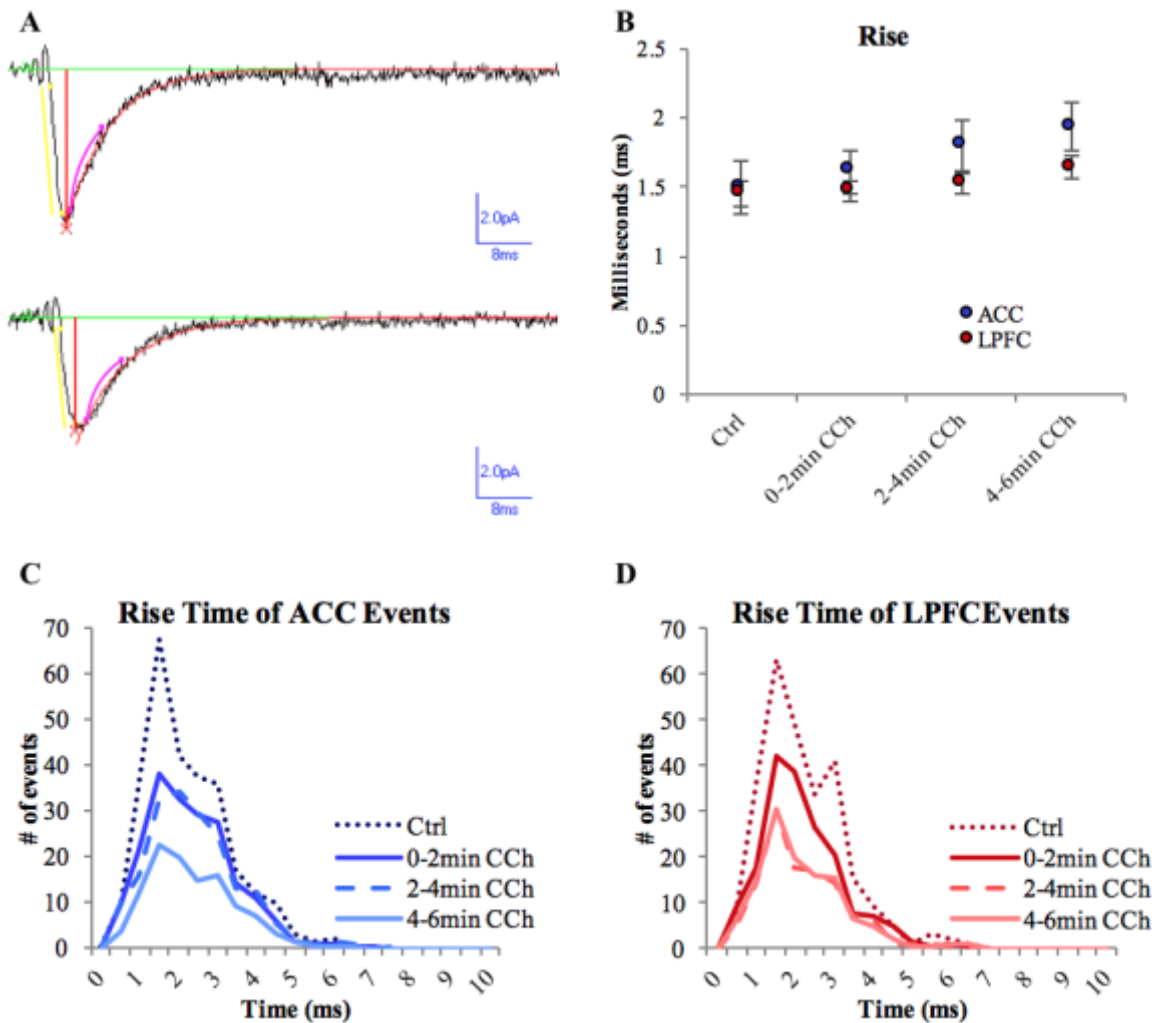


Figure 7. Effects of carbachol on the rise-time of sEPSCs in ACC versus LPFC neurons. (A) Example of sEPSC trace with the yellow line indicating rise-time, pink line marking decay time, and the red line showing amplitude. (B) Mean rise-times across Ctrl, 0-2 min CCh, 2-4 min CCh, and 4-6 min CCh groups comparing the ACC (blue) and the LPFC (red). Population distribution of sEPSCs events' rise-times illustrating CCh's effects on the ACC (C) and LPFC (D).

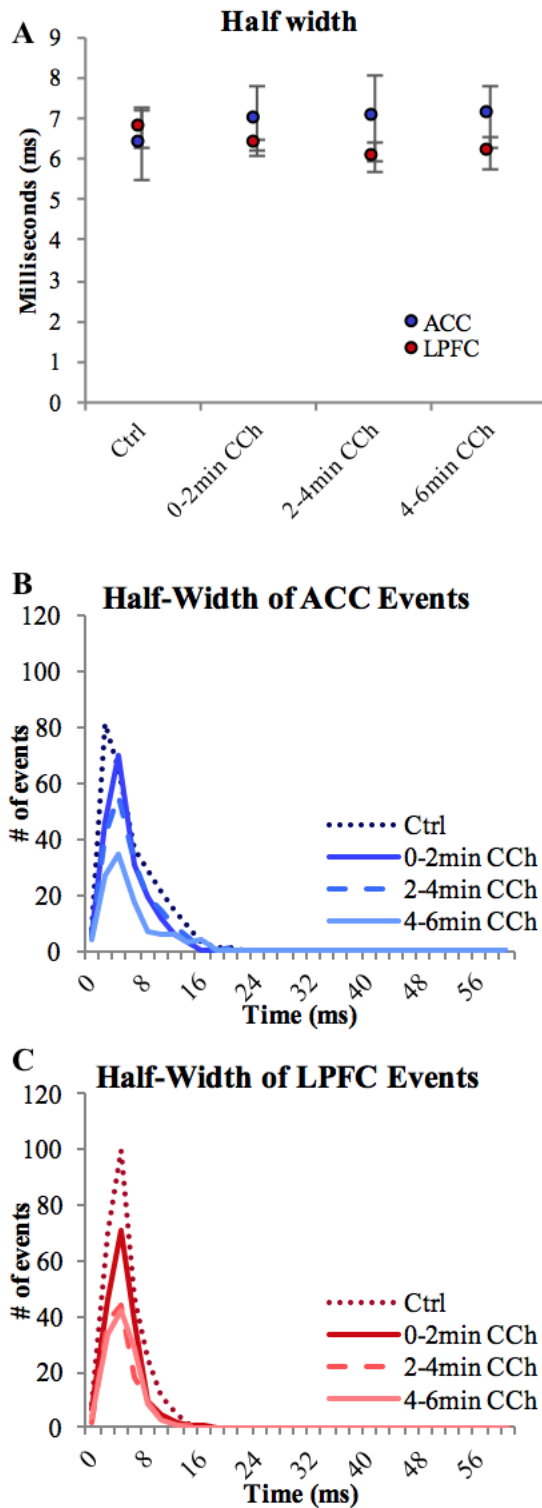


Figure 8. Effects of carbachol on the half-width of sEPSCs in ACC versus LPFC neurons. (A) Mean half-width times for Ctrl, 0-2 min CCh, 2-4 min CCh, and 4-6 min CCh comparing the ACC (blue) and LPFC (red). Population distribution of sEPSCs events' half-width time displaying the effects of CCh for the ACC (B) and the LPFC (C)

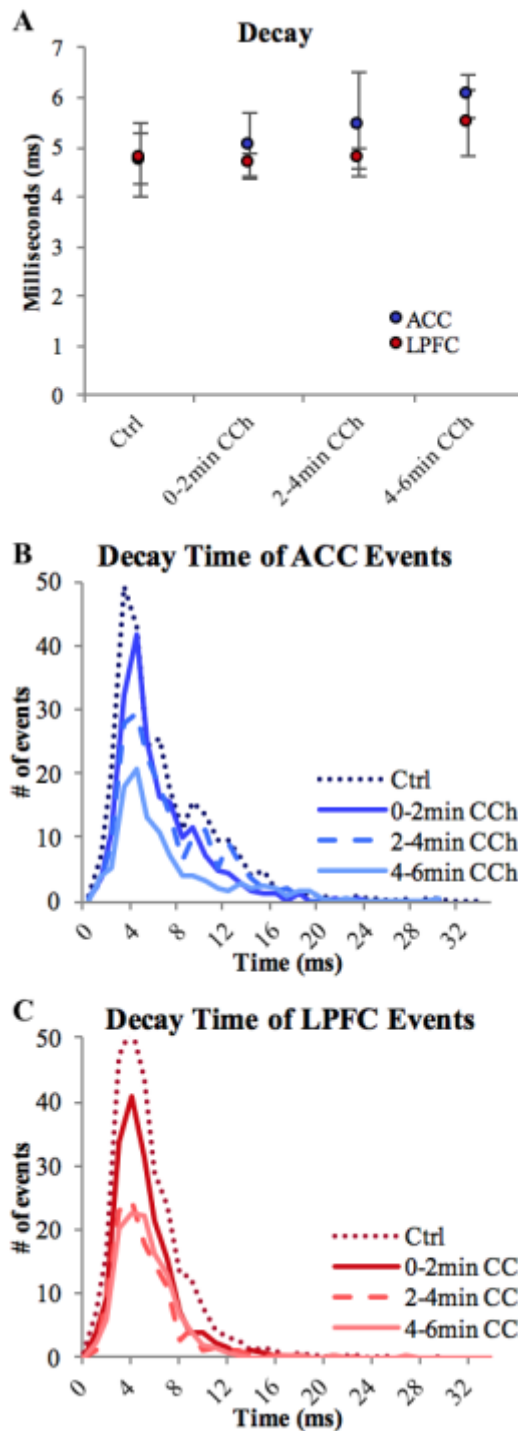


Figure 9. Effects of carbachol on the decay time of sEPSCs in ACC versus LPFC neurons. (A) Mean decay times for Ctrl, 0-2 min CCh, 2-4 min CCh, and 4-6 min CCh comparing the ACC (blue) and LPFC (red). Population distribution of sEPSCs events' decay time displaying the effects of CCh for the ACC (B) and the LPFC (C).

Particle analysis of M2 expression with colocalization of VGLUT1 in the ACC and LPFC

To investigate the possible anatomical basis of cholinergic modulation of excitatory synapses, we looked at the expression of the cholinergic muscarinic receptor, M2 in the ACC and LPFC. This expression level was quantified as the fraction of the sampled field (% area) labeled with M2. We also quantified the extent (% area) of colocalization of M2 receptors with VGLUT1, a marker for presynaptic boutons in the cortex (Figures 10 & 11). We looked at LI and LII-III to compare the differences of the ACC with the LPFC. For LI, there was a significant difference in the total area of M2 label between the ACC and LPFC with the ACC displaying a greater area of M2+ signal than the LPFC (Figure 12A). LII-III did not show a difference between the ACC and LPFC with regards to the total area of M2 label (Figure 12A).

Total area of VGLUT1 label did not differ between the ACC and LPFC in either LI or LII-III (Figure 12B). We did observe a trend ($p = 0.1$) of a larger area of colocalization between M2 and VGLUT1 in LII-III in the ACC and the LPFC. LI did not display any significant difference in the area of M2 and VGLUT1 colocalization between the ACC and LPFC (Figure 12C). M2 positive signal (M2+) and VGLUT1 positive signal (VGLUT1+) colocalization area *versus* total area of VGLUT1+ expression did not show significant difference between the ACC and LPFC in either LI or LII-III (Figure 12D).

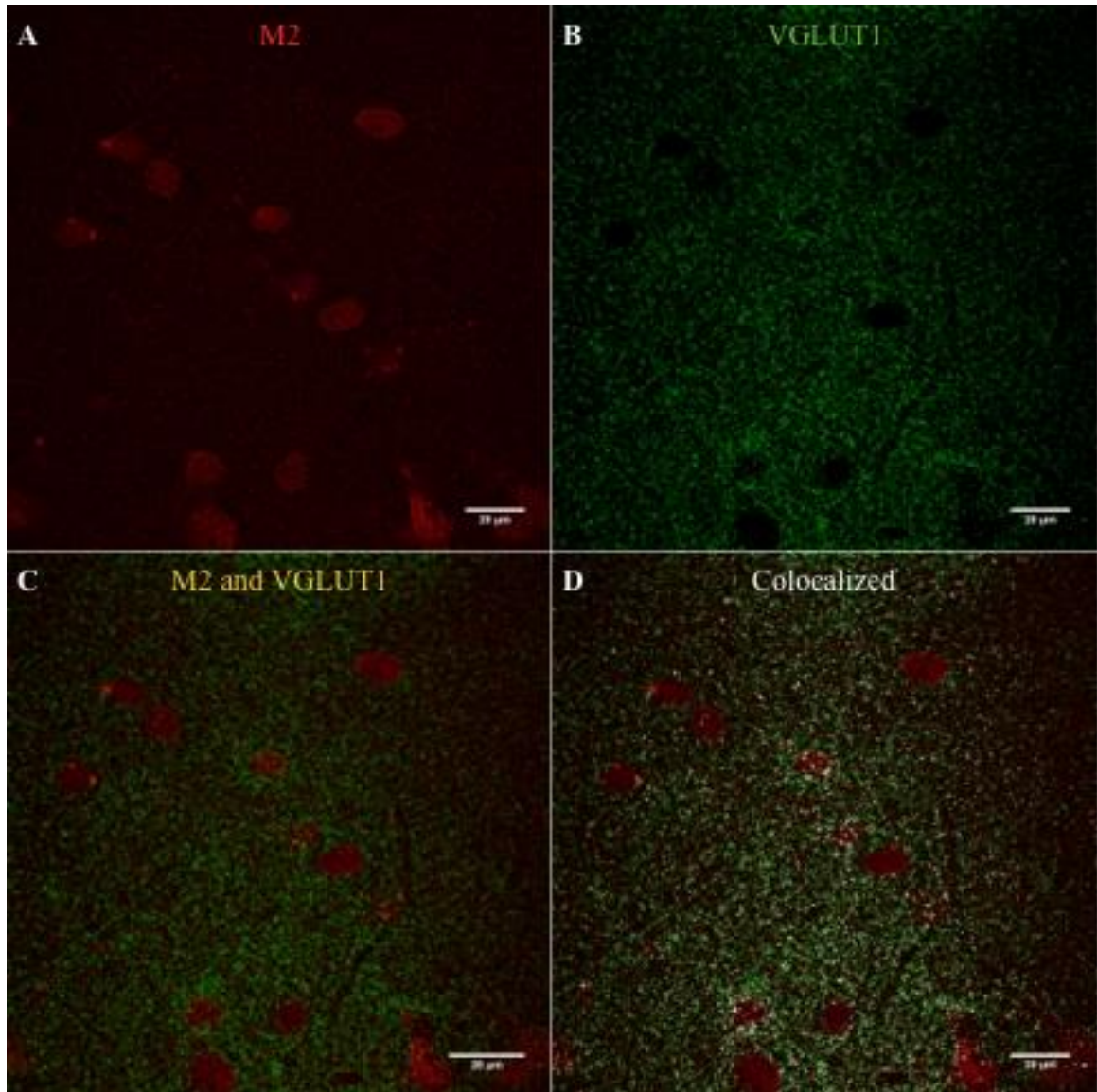


Figure 10. ACC M2 and VGLUT1 expression. Area 24 of the ACC showing M2 expression (A) and VGLUT1 expression (B). (C) M2 and VGLUT1 channels merged to illustrate overlap. (D) The M2 and VGLUT1 channels merged with colocalization represented by the white dots.

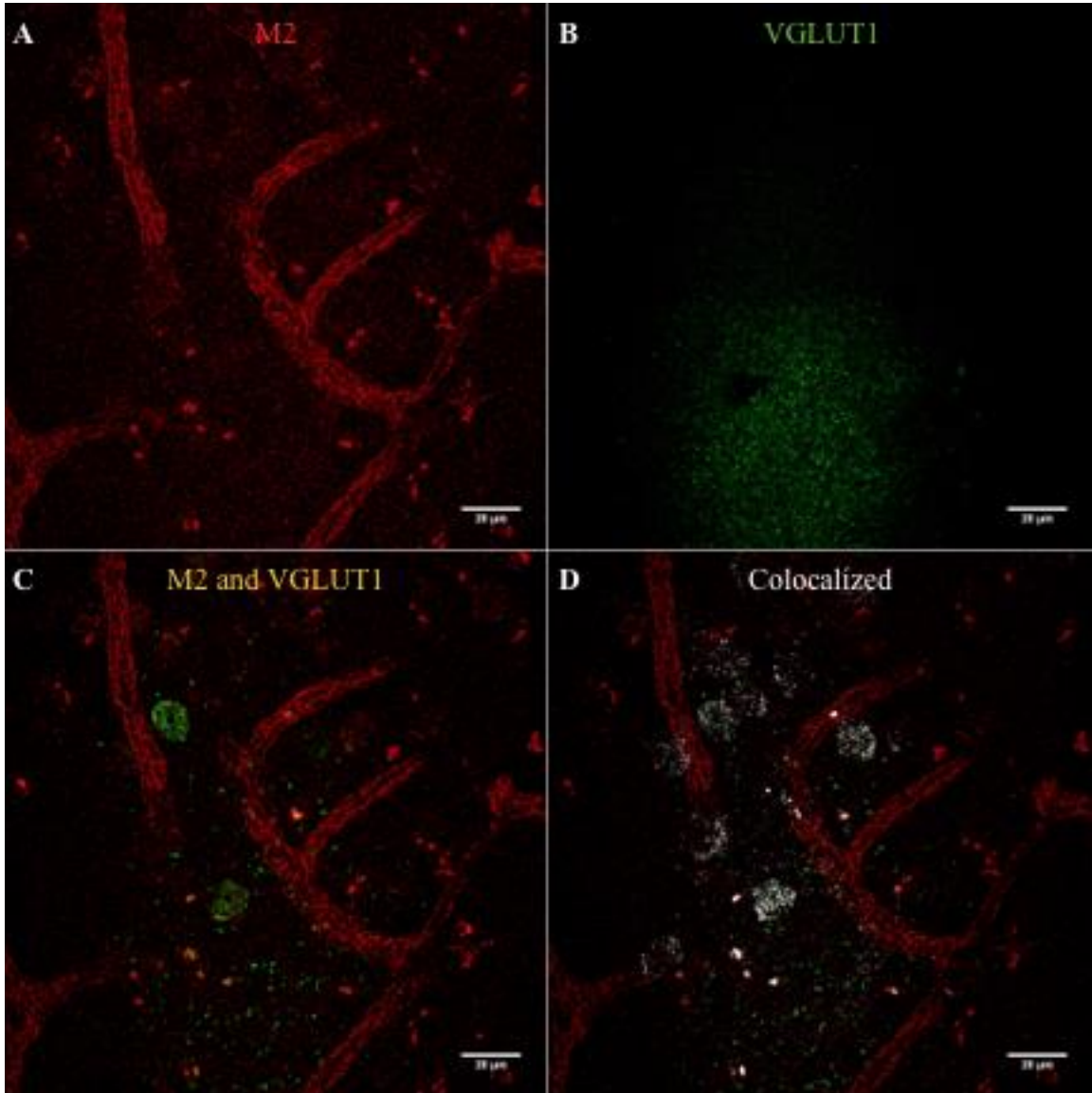


Figure 11. LPFC M2 and VGLUT1 expression. Area 46 of the ACC showing M2 expression (A) and VGLUT1 expression (B). (C) M2 and VGLUT1 channels merged to illustrate overlap. (D) The M2 and VGLUT1 channels merged with colocalization represented by the white dots.

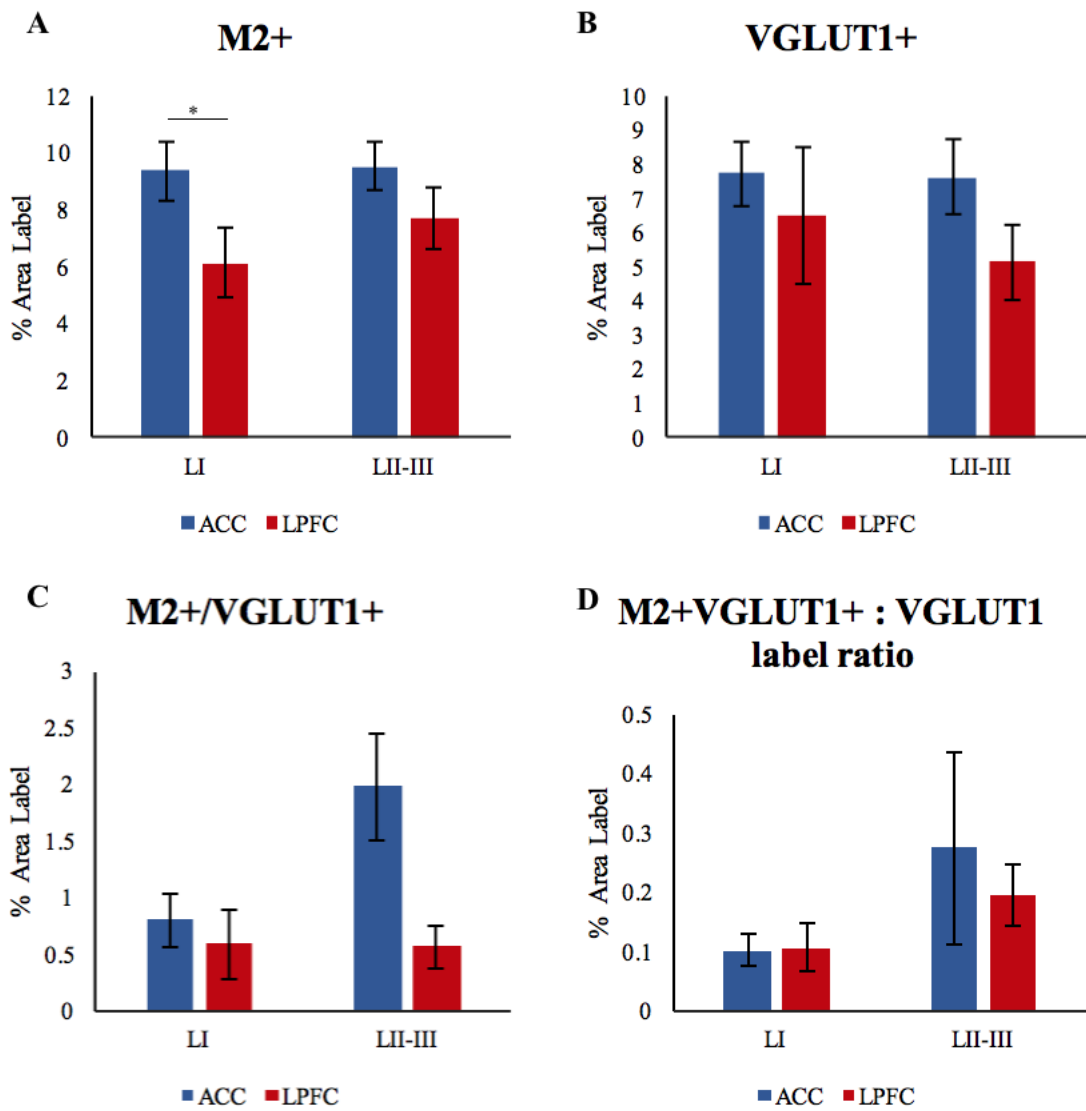


Figure 12. Particle analysis of VGLUT colocalization with M2 expression in the ACC and LPFC. (A) General M2 expression in the ACC *versus* LPFC between LI and LII-III. (B) General VGLUT1 expression in the ACC *versus* LPFC between LI and LII-III. (C) M2+ and VGLUT1+ colocalized regions in the ACC *versus* LPFC between LI and LII-III. (D) Ratio of M2+ & VGLUT+ with total VGLUT1 expression in the ACC *versus* LPFC between LI and LII-III.

Confocal Analysis of Amygdala and Premotor pathways in the ACC

FR tracer was injected into the basolateral nucleus of the amygdala (AMY) to fluoresce projections in area 24 (Figure 13). The confocal analysis of the presence of M2 receptors on amygdala projections was performed on two primate subjects, cases PIJ & PIK (Figures 14 & 15). Imaging and analysis were performed on layers LI-LIII. For case PIK, there was an even distribution of fibers across the four layers, with the highest concentration of projections from the amygdala in LIII (Figure 16B). LIII also was the only layer in case PIK which displayed any colocalization of M2+ with projections from the amygdala.

The distribution of boutons in the AMY pathway of PIJ was predominantly in LI-LIII (~78%) (Figure 16A). We only observed M2 colocalization in LI-II and LII-III, but the percentage of colocalization remained very low (Figure 16B). The higher concentrations of M2+ boutons in the upper layers corresponded with a greater distribution of total fibers on PIJ being in the LI-II and LII-III (Figure 16B).

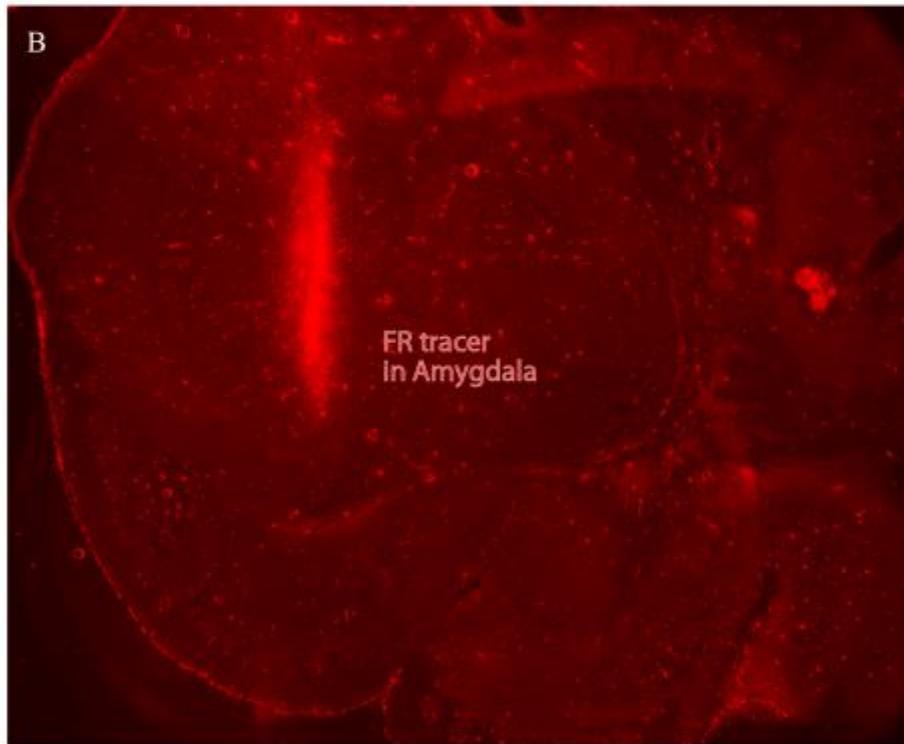
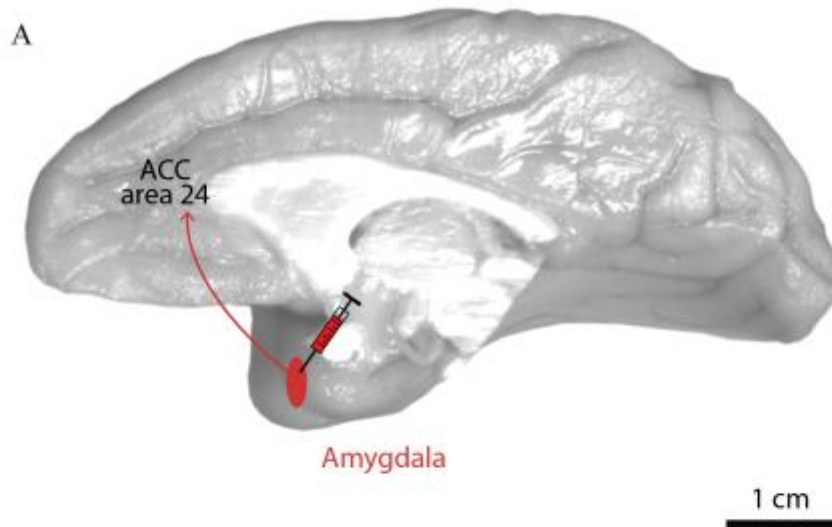


Figure 13. Tracer injection site in amygdala to label projection terminations in the ACC. (A) Medial view of rhesus monkey brain illustrating the injection site in the amygdala with the red arrow showing the terminations of the projections in area 24 of the ACC. (B) Coronal section through the amygdala with fluororuby (FR) tracer injected in the basolateral nucleus. Image from Dr. Maria Medalla

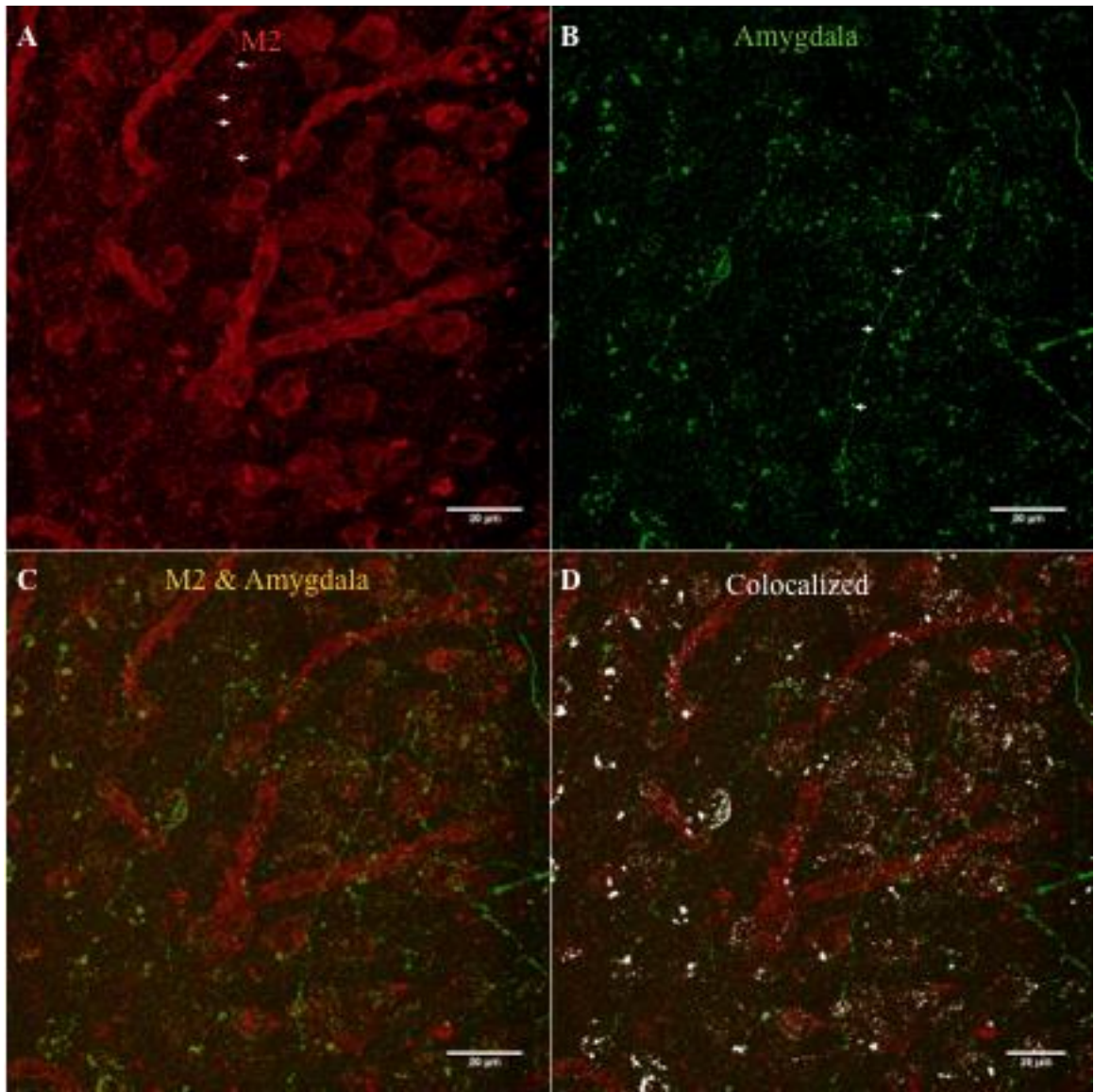


Figure 14. Confocal image of M2 and amygdala fiber in ACC of case PIJ. (A) Fibers expressing M2 in area 24 of the ACC indicated by white arrows. (B) Fibers from amygdala neurons projecting into area 24 of the ACC, indicated by white arrows. (C) M2 and Amygdala channels merged to illustrated overlap. (D) The M2 and amygdala channels merged with colocalization represented by the white dots.

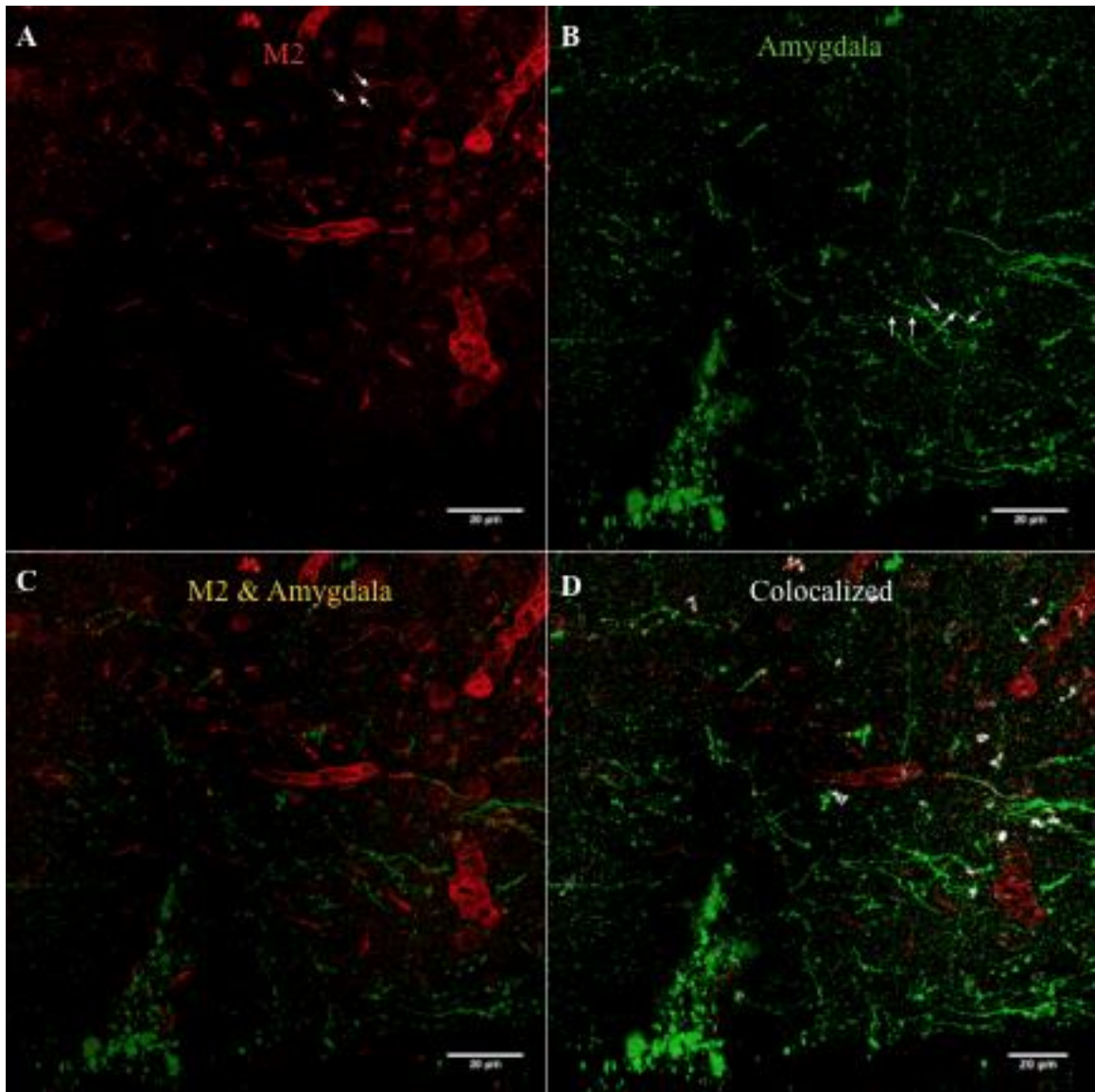


Figure 15. Confocal images of M2 and amygdala fibers in ACC of case PIK. (A) Fibers expressing M2 in area 24 of the ACC indicated by white arrows. (B) Fibers from amygdala neurons projecting into area 24 of the ACC, indicated by white arrows. (C) M2 and Amygdala channels merged to illustrate overlap. (D) The M2 and amygdala channels merged with colocalization represented by the white dots.

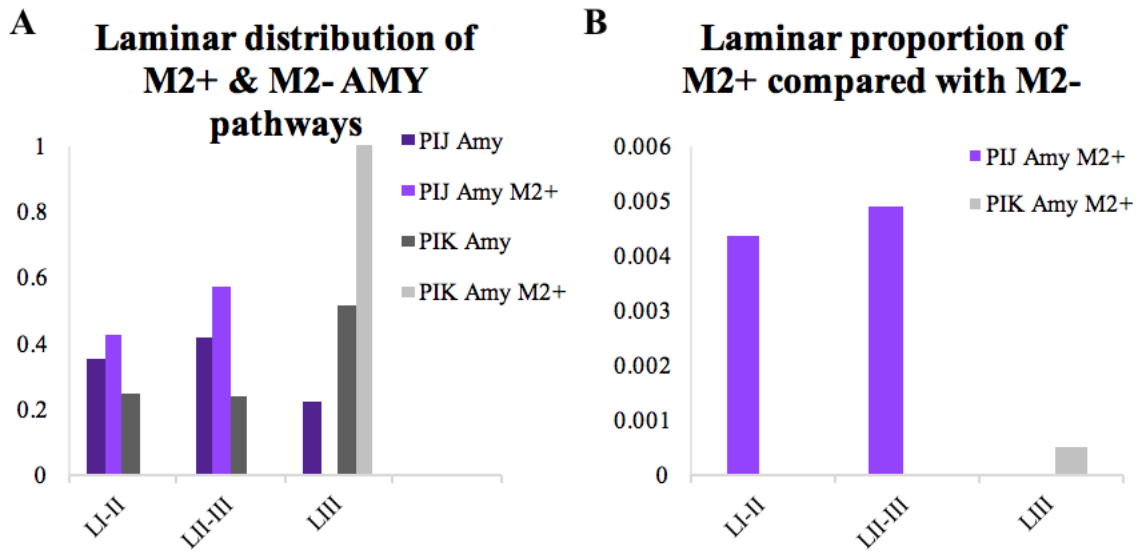


Figure 16. Distribution of amygdala fibers in the ACC. (A) Laminar proportion of total M2 expressing boutons from the amygdala terminating in the ACC from two cases, expressed as a percentage of the total boutons in layers 1-3. (B) Proportion of amygdala boutons terminating in the ACC that are also M2+ in each layer, expressed as a percentage of the total in each layer.

DISCUSSION

The purpose of the study was to understand the action of ACh on pyramidal neurons in two prefrontal areas -- the ACC and LPFC – in rhesus monkeys. ACh plays an important role in memory, learning, and cognition (Hasselmo & Schnell, 1994; Hasselmo & McGaughy, 2004). Specifically, we studied the effect of CCh on the sEPSCs in layer 3 pyramidal neurons of ACC and LPFC. The sEPSCs recorded are the AP-dependent and AP-independent inward cationic currents that result from the binding of glutamate released from the presynaptic terminal to AMPA receptors on the postsynaptic membrane (Hestrin, 1993; Kandel et al., 2012). The flow of cations across the postsynaptic membrane creates a current, which we can measure using whole cell patch-clamp and voltage clamp recording techniques, by holding the neuron at -80mV when the electrochemical driving force for these AMPA currents are high. Thus, we studied the changes in the properties of these sEPSCs after application of the cholinergic agonist CCh. Acetylcholine is known to act directly on the pre or postsynaptic sites of glutamatergic synapses (Peralta et al., 1988; Levey et al., 1991).

The results from the electrophysiological experiments did not reveal significant changes in the amplitude, area, half-width, decay, or rise-time of the sEPSCs due to CCh over time. Therefore, CCh does not appear to affect the gating kinetics of excitatory synaptic currents. There was also no significant difference between the ACC and LPFC cells with respect to these synaptic parameters.

We observed a significant difference in the frequency of sEPSC in both ACC and LPFC with CCh application. The cells from the ACC showed a decrease in frequency

when comparing the control group with 4-6 min CCh group. This was additionally shown using a K-S test for the IEI which displayed a low probability of overlap of event interval distribution when comparing the control with the 4-6 min CCh group for both the ACC and LPFC. The LPFC also showed a decrease in frequency when comparing the control group with the 2-4 min CCh group and the 4-6 min CCh group. The change in frequency after CCh application occurs earlier in LPFC compared to ACC neurons.

We did not observe changes in the amplitude or kinetics of sEPSCs but observed changes in frequency of sEPSCs due to CCh application. This suggests that CCh acts presynaptically on the glutamatergic terminals. The decreased frequency of events indicates a reduced number of glutamate-containing vesicles released into the synaptic cleft by the presynaptic terminal, and suggests a probable mechanism of inhibition by ACh occurring at the presynaptic terminal. This likely involves the M2 muscarinic ACh receptor, which is located on presynaptic terminals (Peralta et al., 1988; Levey et al., 1991). Activation of this receptor directly decreases the probability of release of neurotransmitter from presynaptic terminals. Another possibility for the observed decrease in frequency of sEPSCs would be the decrease in the firing of presynaptic partners of our recorded neurons. Expression of muscarinic receptors on inhibitory neurons in the ACC or LPFC for instance can increase firing of inhibitory neurons (McCormick & Prince, 1985). If CCh increased the firing of inhibitory neurons, it would reduce the AP firing of excitatory presynaptic partners, and therefore reduce the frequency of glutamate release into the synaptic cleft of our recorded neurons. The effect

of CCh on inhibitory currents and also on AP-independent *versus* AP-dependent sEPSCs would be important to address in future work.

While we found that the effects of CCh on sEPSC frequency occurred earlier in LPFC than ACC, our anatomical results showed a greater concentration of M2 receptors in the ACC *versus* the LPFC in layer 1 and similar concentrations in layers 2-3. It is possible this result could be due to the ACC have a higher percentage of M2 expressed on inhibitory neurons. However, we found that the ACC also has a higher colocalization of M2 on VGLUT1+ boutons compared to LPFC. VGLUT transporters are critical in the recycling of glutamine, conversion of glutamine to glutamate, and the packaging of glutamate into vesicles (Fremeau Jr et al., 2004; Shigeri et al., 2004). VGLUT 1 has been shown to be present on cortico-cortical projections, and VGLUT 2 is predominantly present on cortico-subcortical projections (Fremeau Jr et al., 2004; Kashani, Betancur, Giros, Hirsch, & El Mestikawy, 2007; Garcia-Marin, Ahmed, Afzal, & Hawken, 2013). Thus, it is possible that there are other presynaptic muscarinic receptors, such as the M4 subtype, expressed on excitatory terminals and involved in the suppression of sEPSCs in LPFC (Guo, Mao, & Wang, 2010). Future studies using specific receptor blockers in slices and staining of other cholinergic receptors and VGLUTs will be important to understand these differences in cholinergic modulation between ACC and LPFC. It is also likely that since we are using somatic whole-cell patch-clamp recording techniques and the higher M2 expression in ACC compared to LPFC is mainly in layer 1, we are not recording these events which are far from the soma (Golding & Spruston, 1998). We

would need to employ dendritic patch clamp techniques to see if ACC pyramidal neurons apical dendrites in layer 1 are more modulated by ACh compared to LPFC.

For the analysis of specific pathway interactions with M2 receptors, we looked at amygdala projections to the ACC. Since the ACC is part of the Papez limbic circuit, we wanted to observe the projections from one limbic area to another. The limbic circuit, which is heavily innervated by cholinergic fibers, includes the amygdala which has been shown to have muscarinic and nicotinic receptors in the rat (Hecker & Mesulam, 1994; Jiang et al., 2016; Wilson & Fadel, 2017). In both animals, there was no significant presence of M2 expression on fibers projecting from the amygdala terminating in the ACC. This suggests that ACh likely does not suppress this specific pathway. This is interesting because during rest, the CNS receives an influx of acetylcholine from the basal nuclei which helps increase the signal to noise ratio, necessary for memory consolidation (Bunce et al., 2004; Elvander et al., 2004; Michael E Hasselmo, 2006). Strong activation of the limbic circuit is needed for this process, and it seems that ACh allows the limbic circuit activation to be dominant during memory consolidation.

In summary, our data show that ACh decreases the frequency of excitatory synaptic events in two prefrontal areas in primates. But the time course and potential mechanisms are different. Moreover, the circuits involved and modulated by ACh appear to vary depending on the layer and area. Future work would be important to further address these different mechanisms and pathway properties in the primate ACC *versus* LPFC.

REFERENCES

- Alexander, G. E., DeLong, M. R., & Strick, P. L. (1986). Parallel organization of functionally segregated circuits linking basal ganglia and cortex. *Annual Review of Neuroscience*, 9, 357–381.
<https://doi.org/10.1146/annurev.ne.09.030186.002041>
- Amatrudo, J. M., Weaver, C. M., Crimins, J. L., Hof, P. R., Rosene, D. L., & Luebke, J. I. (2012). Influence of Highly Distinctive Structural Properties on the Excitability of Pyramidal Neurons in Monkey Visual and Prefrontal Cortices. *Journal of Neuroscience*, 32(40), 13644–13660. <https://doi.org/10.1523/JNEUROSCI.2581-12.2012>
- Andersen, R. A., Asanuma, C., Essick, G., & Siegel, R. M. (1990). Corticocortical connections of anatomically and physiologically defined subdivisions within the inferior parietal lobule. *The Journal of Comparative Neurology*, 296(1), 65–113.
<https://doi.org/10.1002/cne.902960106>
- Aston-Jones, G., & Cohen, J. D. (2005). Adaptive gain and the role of the locus coeruleus-norepinephrine system in optimal performance. *The Journal of Comparative Neurology*, 493(1), 99–110. <https://doi.org/10.1002/cne.20723>
- Barbas, H. (2000). Complementary roles of prefrontal cortical regions in cognition, memory, and emotion in primates. *Advances in Neurology*, 84, 87–110.
- Barbas, H. (2015). General cortical and special prefrontal connections: principles from structure to function. *Annual Review of Neuroscience*, 38, 269–289.
<https://doi.org/10.1146/annurev-neuro-071714-033936>

- Barbas, H., & Blatt, G. J. (1995). Topographically specific hippocampal projections target functionally distinct prefrontal areas in the rhesus monkey. *Hippocampus*, 5(6), 511–533. <https://doi.org/10.1002/hipo.450050604>
- Barbas, H., & De Olmos, J. (1990). Projections from the amygdala to basoventral and mediodorsal prefrontal regions in the rhesus monkey. *The Journal of Comparative Neurology*, 300(4), 549–571. <https://doi.org/10.1002/cne.903000409>
- Barbas, H., & Pandya, D. (1989). Architecture and Intrinsic Connections of the Prefrontal Cortex in the Rhesus-Monkey. *Journal of Comparative Neurology*, 286(3), 353–375. <https://doi.org/10.1002/cne.902860306>
- Barbas, H., & Zikopoulos, B. (2007). The prefrontal cortex and flexible behavior. *The Neuroscientist: A Review Journal Bringing Neurobiology, Neurology and Psychiatry*, 13(5), 532–545. <https://doi.org/10.1177/1073858407301369>
- Bates, J., & Goldmanrakis, P. (1993). Prefrontal Connections of Medial Motor Areas in the Rhesus-Monkey. *Journal of Comparative Neurology*, 336(2), 211–228. <https://doi.org/10.1002/cne.903360205>
- Berger, B. (1992). Dopaminergic innervation of the frontal cerebral cortex. Evolutionary trends and functional implications. *Advances in Neurology*, 57, 525–544.
- Brunia, C. H. M., Haagh, S. a. V. M., & Scheirs, J. G. M. (1985). Waiting to Respond: Electrophysiological Measurements in Man During Preparation for a Voluntary Movement. In P. D. H. Heuer, P. D. U. Kleinbeck, & D.-P. K.-H. Schmidt (Eds.), *Motor Behavior* (pp. 35–78). Springer Berlin Heidelberg. https://doi.org/10.1007/978-3-642-69749-4_2

- Bunce, J. G., Sabolek, H. R., & Chrobak, J. J. (2004). Intraseptal infusion of the cholinergic agonist carbachol impairs delayed-non-match-to-sample radial arm maze performance in the rat. *Hippocampus*, *14*(4), 450–459. <https://doi.org/10.1002/hipo.10200>
- Carmichael, S. T., & Price, J. L. (1995). Sensory and premotor connections of the orbital and medial prefrontal cortex of macaque monkeys. *The Journal of Comparative Neurology*, *363*(4), 642–664. <https://doi.org/10.1002/cne.903630409>
- Cavada, C., & Goldman-Rakic, P. S. (1989). Posterior parietal cortex in rhesus monkey: II. Evidence for segregated corticocortical networks linking sensory and limbic areas with the frontal lobe. *The Journal of Comparative Neurology*, *287*(4), 422–445. <https://doi.org/10.1002/cne.902870403>
- Chang, F. L., & Greenough, W. T. (1984). Transient and enduring morphological correlates of synaptic activity and efficacy change in the rat hippocampal slice. *Brain Research*, *309*(1), 35–46.
- Chrobak, J. J., & Buzsáki, G. (1994). Selective activation of deep layer (V-VI) retrohippocampal cortical neurons during hippocampal sharp waves in the behaving rat. *The Journal of Neuroscience: The Official Journal of the Society for Neuroscience*, *14*(10), 6160–6170.
- Corkin, S. (1979). Hidden-figures-test performance: lasting effects of unilateral penetrating head injury and transient effects of bilateral cingulotomy. *Neuropsychologia*, *17*(6), 585–605.

- Defelipe, J. (2011). The evolution of the brain, the human nature of cortical circuits, and intellectual creativity. *Frontiers in Neuroanatomy*, 5, 29.
<https://doi.org/10.3389/fnana.2011.00029>
- DeFelipe, J., & Fariñas, I. (1992). The pyramidal neuron of the cerebral cortex: morphological and chemical characteristics of the synaptic inputs. *Progress in Neurobiology*, 39(6), 563–607.
- Devinsky, O., Morrell, M. J., & Vogt, B. A. (1995). Contributions of anterior cingulate cortex to behaviour. *Brain: A Journal of Neurology*, 118 (Pt 1), 279–306.
- Douglas, R. J., & Martin, K. A. C. (2004). Neuronal circuits of the neocortex. *Annual Review of Neuroscience*, 27, 419–451.
<https://doi.org/10.1146/annurev.neuro.27.070203.144152>
- Dum, R. P., & Strick, P. L. (1991). The origin of corticospinal projections from the premotor areas in the frontal lobe. *The Journal of Neuroscience: The Official Journal of the Society for Neuroscience*, 11(3), 667–689.
- Dunnett, S., Everitt, B., & Robbins, T. (1991). The Basal Forebrain Cortical Cholinergic System - Interpreting the Functional Consequences of Excitotoxic Lesions. *Trends in Neurosciences*, 14(11), 494–501. [https://doi.org/10.1016/0166-2236\(91\)90061-X](https://doi.org/10.1016/0166-2236(91)90061-X)
- Elston, G. N. (2003). Cortex, cognition and the cell: new insights into the pyramidal neuron and prefrontal function. *Cerebral Cortex (New York, N.Y.: 1991)*, 13(11), 1124–1138.

- Elvander, E., Schött, P. A., Sandin, J., Bjelke, B., Kehr, J., Yoshitake, T., & Ogren, S. O. (2004). Intraseptal muscarinic ligands and galanin: influence on hippocampal acetylcholine and cognition. *Neuroscience*, *126*(3), 541–557.
<https://doi.org/10.1016/j.neuroscience.2004.03.058>
- Everitt, B. J., & Robbins, T. W. (1997). Central cholinergic systems and cognition. *Annual Review of Psychology*, *48*, 649–684.
<https://doi.org/10.1146/annurev.psych.48.1.649>
- Fremeau Jr, R. T., Voglmaier, S., Seal, R. P., & Edwards, R. H. (2004). VGLUTs define subsets of excitatory neurons and suggest novel roles for glutamate. *Trends in Neurosciences*, *27*(2), 98–103. <https://doi.org/10.1016/j.tins.2003.11.005>
- Funahashi, S., Bruce, C., & Goldmanrakis, P. (1989). Mnemonic Coding of Visual Space in the Monkeys Dorsolateral Prefrontal Cortex. *Journal of Neurophysiology*, *61*(2), 331–349.
- Funahashi, S., Bruce, C., & Goldmanrakis, P. (1993). Dorsolateral Prefrontal Lesions and Oculomotor Delayed-Response Performance - Evidence for Mnemonic Scotomas. *Journal of Neuroscience*, *13*(4), 1479–1497.
- Fuster, J. M. (2001). The prefrontal cortex--an update: time is of the essence. *Neuron*, *30*(2), 319–333.
- Garcia-Marin, V., Ahmed, T. H., Afzal, Y. C., & Hawken, M. J. (2013). Distribution of Vesicular Glutamate Transporter 2 (VGluT2) in the Primary Visual Cortex of the Macaque and Human. *The Journal of Comparative Neurology*, *521*(1), 130–151.
<https://doi.org/10.1002/cne.23165>

- Golding, N. L., & Spruston, N. (1998). Dendritic sodium spikes are variable triggers of axonal action potentials in hippocampal CA1 pyramidal neurons. *Neuron*, *21*(5), 1189–1200.
- Goldman-Rakic, P. S. (1995). Cellular basis of working memory. *Neuron*, *14*(3), 477–485.
- Goodfellow, N. M., Benekareddy, M., Vaidya, V. A., & Lambe, E. K. (2009). Layer II/III of the Prefrontal Cortex: Inhibition by the Serotonin 5-HT_{1A} Receptor in Development and Stress. *Journal of Neuroscience*, *29*(32), 10094–10103.
<https://doi.org/10.1523/JNEUROSCI.1960-09.2009>
- Guerram, M., Zhang, L.-Y., & Jiang, Z.-Z. (2016). G-protein coupled receptors as therapeutic targets for neurodegenerative and cerebrovascular diseases. *Neurochemistry International*, *101*, 1–14.
<https://doi.org/10.1016/j.neuint.2016.09.005>
- GUO, M.-L., MAO, L.-M., & WANG, J. Q. (2010). Modulation of M₄ muscarinic acetylcholine receptors by interacting proteins. *Neuroscience Bulletin*, *26*(6), 469–473.
- Hamberger, A. C., Chiang, G. H., Nylén, E. S., Scheff, S. W., & Cotman, C. W. (1979). Glutamate as a CNS transmitter. I. Evaluation of glucose and glutamine as precursors for the synthesis of preferentially released glutamate. *Brain Research*, *168*(3), 513–530.
- Hasselmo, null. (1999). Neuromodulation: acetylcholine and memory consolidation. *Trends in Cognitive Sciences*, *3*(9), 351–359.

- Hasselmo, M. E. (1995). Neuromodulation and cortical function: modeling the physiological basis of behavior. *Behavioural Brain Research*, 67(1), 1–27.
- Hasselmo, M. E. (2006). The role of acetylcholine in learning and memory. *Current Opinion in Neurobiology*, 16(6), 710–715.
<https://doi.org/10.1016/j.conb.2006.09.002>
- Hasselmo, M. E., & McGaughy, J. (2004). High acetylcholine levels set circuit dynamics for attention and encoding and low acetylcholine levels set dynamics for consolidation. In L. Descarries, K. Krnjevic, & M. Steriade (Eds.), *Acetylcholine in the Cerebral Cortex* (Vol. 145, pp. 207–231). Amsterdam: Elsevier Science Bv.
- Hasselmo, M. E., & Schnell, E. (1994). Laminar selectivity of the cholinergic suppression of synaptic transmission in rat hippocampal region CA1: computational modeling and brain slice physiology. *The Journal of Neuroscience: The Official Journal of the Society for Neuroscience*, 14(6), 3898–3914.
- Hecker, S., & Mesulam, M. M. (1994). Two types of cholinergic projections to the rat amygdala. *Neuroscience*, 60(2), 383–397.
- Hering, H., & Sheng, M. (2001). Dendritic spines : structure, dynamics and regulation. *Nature Reviews Neuroscience*, 2(12), 880–888. <https://doi.org/10.1038/35104061>
- Hessler, N. A., Shirke, A. M., & Malinow, R. (1993). The probability of transmitter release at a mammalian central synapse. *Nature*, 366(6455), 569–572.
<https://doi.org/10.1038/366569a0>

- Hestrin, S. (1993). Different Glutamate-Receptor Channels Mediate Fast Excitatory Synaptic Currents in Inhibitory and Excitatory Cortical-Neurons. *Neuron*, *11*(6), 1083–1091. [https://doi.org/10.1016/0896-6273\(93\)90221-C](https://doi.org/10.1016/0896-6273(93)90221-C)
- Jenkins, I., Brooks, D., Nixon, P., Frackowiak, R., & Passingham, R. (1994). Motor Sequence Learning - a Study with Positron Emission Tomography. *Journal of Neuroscience*, *14*(6), 3775–3790.
- Jiang, L., Kundu, S., Lederman, J. D., López-Hernández, G. Y., Ballinger, E. C., Wang, S., ... Role, L. W. (2016). Cholinergic Signaling Controls Conditioned Fear Behaviors and Enhances Plasticity of Cortical-Amygdala Circuits. *Neuron*, *90*(5), 1057–1070. <https://doi.org/10.1016/j.neuron.2016.04.028>
- Jones, E. G. (1998). Viewpoint: the core and matrix of thalamic organization. *Neuroscience*, *85*(2), 331–345. [https://doi.org/10.1016/S0306-4522\(97\)00581-2](https://doi.org/10.1016/S0306-4522(97)00581-2)
- Kandel, E. R., Schwartz, J. H., Jessell, T. M., Siegelbaum, S. A., & Hudspeth, A. J. (Eds.). (2012). *Principles of Neural Science, Fifth Edition* (5th edition). New York: McGraw-Hill Education / Medical.
- Kashani, A., Betancur, C., Giros, B., Hirsch, E., & El Mestikawy, S. (2007). Altered expression of vesicular glutamate transporters VGLUT1 and VGLUT2 in Parkinson disease. *Neurobiology of Aging*, *28*(4), 568–578. <https://doi.org/10.1016/j.neurobiolaging.2006.02.010>
- Kennard, M. A. (1955). Effect of bilateral ablation of cingulate area on behaviour of cats. *Journal of Neurophysiology*, *18*(2), 159–169.

- Krnjević, K., & Phillis, J. W. (1963). Acetylcholine-sensitive cells in the cerebral cortex. *The Journal of Physiology*, *166*(2), 296–327.
- Krnjević, K., Pumain, R., & Renaud, L. (1971). The mechanism of excitation by acetylcholine in the cerebral cortex. *The Journal of Physiology*, *215*(1), 247–268.
- Levey, A. I., Kitt, C. A., Simonds, W. F., Price, D. L., & Brann, M. R. (1991). Identification and localization of muscarinic acetylcholine receptor proteins in brain with subtype-specific antibodies. *The Journal of Neuroscience: The Official Journal of the Society for Neuroscience*, *11*(10), 3218–3226.
- Luebke, J., Barbas, H., & Peters, A. (2010). Effects of normal aging on prefrontal area 46 in the rhesus monkey. *Brain Research Reviews*, *62*(2), 212–232.
<https://doi.org/10.1016/j.brainresrev.2009.12.002>
- Luebke, J. I., & Amatrudo, J. M. (2012). Age-related increase of sIAHP in prefrontal pyramidal cells of monkeys: relationship to cognition. *Neurobiology of Aging*, *33*(6), 1085–1095. <https://doi.org/10.1016/j.neurobiolaging.2010.07.002>
- Luppino, G., Matelli, M., Camarda, R. M., Gallese, V., & Rizzolatti, G. (1991). Multiple representations of body movements in mesial area 6 and the adjacent cingulate cortex: an intracortical microstimulation study in the macaque monkey. *The Journal of Comparative Neurology*, *311*(4), 463–482.
<https://doi.org/10.1002/cne.903110403>
- Markram, H., Toledo-Rodriguez, M., Wang, Y., Gupta, A., Silberberg, G., & Wu, C. Z. (2004). Interneurons of the neocortical inhibitory system. *Nature Reviews Neuroscience*, *5*(10), 793–807. <https://doi.org/10.1038/nrn1519>

- McCormick, D. A., & Prince, D. A. (1985). Two types of muscarinic response to acetylcholine in mammalian cortical neurons. *Proceedings of the National Academy of Sciences of the United States of America*, 82(18), 6344–6348.
- McKinney, M. (1993). Muscarinic receptor subtype-specific coupling to second messengers in neuronal systems. *Progress in Brain Research*, 98, 333–340.
- Medalla, M., & Barbas, H. (2009). Synapses with inhibitory neurons differentiate anterior cingulate from dorsolateral prefrontal pathways associated with cognitive control. *Neuron*, 61(4), 609–620. <https://doi.org/10.1016/j.neuron.2009.01.006>
- Medalla, M., & Barbas, H. (2010). Anterior cingulate synapses in prefrontal areas 10 and 46 suggest differential influence in cognitive control. *The Journal of Neuroscience: The Official Journal of the Society for Neuroscience*, 30(48), 16068–16081. <https://doi.org/10.1523/JNEUROSCI.1773-10.2010>
- Medalla, M., & Barbas, H. (2012). The Anterior Cingulate Cortex May Enhance Inhibition of Lateral Prefrontal Cortex Via M2 Cholinergic Receptors at Dual Synaptic Sites. *The Journal of Neuroscience*, 32(44), 15611–15625. <https://doi.org/10.1523/JNEUROSCI.2339-12.2012>
- Medalla, M., Lera, P., Feinberg, M., & Barbas, H. (2007). Specificity in inhibitory systems associated with prefrontal pathways to temporal cortex in primates. *Cerebral Cortex (New York, N.Y.: 1991)*, 17 Suppl 1, i136-150. <https://doi.org/10.1093/cercor/bhm068>
- Mesulam, M., Mufson, E., Levey, A., & Wainer, B. (1983). Cholinergic Innervation of Cortex by the Basal Forebrain - Cyto-Chemistry and Cortical Connections of the

- Septal Area, Diagonal Band Nuclei, Nucleus Basalis (substantia Innominata), and Hypothalamus. *Journal of Comparative Neurology*, 214(2), 170–197.
<https://doi.org/10.1002/cne.902140206>
- Miller, E. K., & Cohen, J. D. (2001). An integrative theory of prefrontal cortex function. *Annual Review of Neuroscience*, 24, 167–202.
<https://doi.org/10.1146/annurev.neuro.24.1.167>
- Muzur, A., Pace-Schott, E. F., & Hobson, J. A. (2002). The prefrontal cortex in sleep. *Trends in Cognitive Sciences*, 6(11), 475–481.
- National Research Council (US) Committee for the Update of the Guide for the Care and Use of Laboratory Animals. (2011). *Guide for the Care and Use of Laboratory Animals* (8th ed.). Washington (DC): National Academies Press (US). Retrieved from <http://www.ncbi.nlm.nih.gov/books/NBK54050/>
- Nicholls, J. G., Martin, A. R., Fuchs, P. A., Brown, D. A., Diamond, M. E., & Weisblat, D. (2011). *From Neuron to Brain, Fifth Edition* (5 edition). Sunderland, Mass: Sinauer Associates, Inc.
- Owen, A., Downes, J., Sahakian, B., Polkey, C., & Robbins, T. (1990). Planning and Spatial Working Memory Following Frontal-Lobe Lesions in Man. *Neuropsychologia*, 28(10), 1021–1034. [https://doi.org/10.1016/0028-3932\(90\)90137-D](https://doi.org/10.1016/0028-3932(90)90137-D)
- Ozkan, E. D., & Ueda, T. (1998). Glutamate transport and storage in synaptic vesicles. *Japanese Journal of Pharmacology*, 77(1), 1–10.

- Pardo, J. V., Pardo, P. J., Janer, K. W., & Raichle, M. E. (1990). The anterior cingulate cortex mediates processing selection in the Stroop attentional conflict paradigm. *Proceedings of the National Academy of Sciences of the United States of America*, 87(1), 256–259.
- Paus, T. (2001). Primate anterior cingulate cortex: Where motor control, drive and cognition interface. *Nature Reviews Neuroscience*, 2(6), 417–424.
<https://doi.org/10.1038/35077500>
- Paus, T., Tomaiuolo, F., Otaky, N., MacDonald, D., Petrides, M., Atlas, J., ... Evans, A. C. (1996). Human cingulate and paracingulate sulci: Pattern, variability, asymmetry, and probabilistic map. *Cerebral Cortex*, 6(2), 207–214.
<https://doi.org/10.1093/cercor/6.2.207>
- Peralta, E. G., Ashkenazi, A., Winslow, J. W., Ramachandran, J., & Capon, D. J. (1988). Differential regulation of PI hydrolysis and adenylyl cyclase by muscarinic receptor subtypes. *Nature*, 334(6181), 434–437. <https://doi.org/10.1038/334434a0>
- Peters, A., & Kaiserman-Abramof, I. R. (1970). The small pyramidal neuron of the rat cerebral cortex. The perikaryon, dendrites and spines. *The American Journal of Anatomy*, 127(4), 321–355. <https://doi.org/10.1002/aja.1001270402>
- Petrides, M. (1994). Functional Specialization Within the Dorsolateral Frontal-Cortex. *Revue De Neuropsychologie*, 4(3), 305–325.
- Petrides, M. (2005). Lateral prefrontal cortex: architectonic and functional organization. *Philosophical Transactions of the Royal Society B: Biological Sciences*, 360(1456), 781–795. <https://doi.org/10.1098/rstb.2005.1631>

- Petrides, M., & Pandya, D. N. (1984). Projections to the frontal cortex from the posterior parietal region in the rhesus monkey. *The Journal of Comparative Neurology*, 228(1), 105–116. <https://doi.org/10.1002/cne.902280110>
- Petrides, M., Tomaiuolo, F., Yeterian, E. H., & Pandya, D. N. (2012). The prefrontal cortex: comparative architectonic organization in the human and the macaque monkey brains. *Cortex; a Journal Devoted to the Study of the Nervous System and Behavior*, 48(1), 46–57. <https://doi.org/10.1016/j.cortex.2011.07.002>
- Posner, M. I., & Dehaene, S. (1994). Attentional networks. *Trends in Neurosciences*, 17(2), 75–79.
- Rasband, W.S., ImageJ, U. S. National Institutes of Health, Bethesda, Maryland, USA, <https://imagej.nih.gov/ij/>, 1997-2016
- Rempel-Clower, N. L., & Barbas, H. (1998). Topographic organization of connections between the hypothalamus and prefrontal cortex in the rhesus monkey. *The Journal of Comparative Neurology*, 398(3), 393–419.
- Rizzolatti, G., Camarda, R., Fogassi, L., Gentilucci, M., Luppino, G., & Matelli, M. (1988). Functional organization of inferior area 6 in the macaque monkey. II. Area F5 and the control of distal movements. *Experimental Brain Research*, 71(3), 491–507.
- Rosene, D. L., Roy, N. J., & Davis, B. J. (1986). A cryoprotection method that facilitates cutting frozen sections of whole monkey brains for histological and histochemical

- processing without freezing artifact. *The Journal of Histochemistry and Cytochemistry: Official Journal of the Histochemistry Society*, 34(10), 1301–1315.
- Rosenmund, C., Clements, J. D., & Westbrook, G. L. (1993). Nonuniform probability of glutamate release at a hippocampal synapse. *Science (New York, N.Y.)*, 262(5134), 754–757.
- Rushworth, M. F. S., Walton, M. E., Kennerley, S. W., & Bannerman, D. M. (2004). Action sets and decisions in the medial frontal cortex. *Trends in Cognitive Sciences*, 8(9), 410–417. <https://doi.org/10.1016/j.tics.2004.07.009>
- Schacter, D. L. (1997). The cognitive neuroscience of memory: perspectives from neuroimaging research. *Philosophical Transactions of the Royal Society of London Series B-Biological Sciences*, 352(1362), 1689–1695.
- Schneider, C.A., Rasband, W.S., Eliceiri, K.W. "NIH Image to ImageJ: 25 years of image analysis". *Nature Methods* 9, 671-675, 2012.
- Shigeri, Y., Seal, R. P., & Shimamoto, K. (2004). Molecular pharmacology of glutamate transporters, EAATs and VGLUTs. *Brain Research Reviews*, 45(3), 250–265. <https://doi.org/10.1016/j.brainresrev.2004.04.004>
- Stuart, G., Schiller, J., & Sakmann, B. (1997). Action potential initiation and propagation in rat neocortical pyramidal neurons. *The Journal of Physiology*, 505 (Pt 3), 617–632.

Wilson, M. A., & Fadel, J. R. (2017). Cholinergic regulation of fear learning and extinction. *Journal of Neuroscience Research*, 95(3), 836–852.
<https://doi.org/10.1002/jnr.23840>

CURRICULUM VITAE

